Effect of Confinement and Gauging on the Performance of MMFX High Strength Reinforcing Bar Tension Lap Splices

by

Kathryn Diane Hoyt, B.S.C.E

Thesis

Presented to the Faculty of the Graduate School of

The University of Texas at Austin

in Partial Fulfillment

of the Requirements

for the Degree of

Master of Science in Engineering

The University of Texas at Austin

May 2007

Effect of Confinement and Gauging on the Performance of MMFX High Strength Reinforcing Bar Tension Lap Splices

Approved by
Supervising Committee:

_____

_____

Dedication

To my parents, my sister Angie, and to Jacob Myers who have offered their unconditional love and support throughout my educational journey.

Acknowledgements

I would like to express my sincere appreciation to my advisor Dr. Jim Jirsa for his guidance and advice. I feel fortunate to have learned from someone who is a world-renowned expert in the field and whose humble and personable nature has made a significant difference in my graduate school experience.

The staff at the Ferguson Structural Engineering Laboratory made the completion of this research possible. Their knowledge and assistance has been greatly appreciated. Also, I would like to extend my thanks to Greg Glass, a fellow graduate student, for his collaboration.

Finally, I offer my deepest gratitude to my family. Their unlimited belief in me makes all things seem possible.

May 2007

Abstract

Effect of Confinement and Gauging on the Performance of MMFX High Strength Reinforcing Bar Tension Lap Splices

Kathryn Diane Hoyt, M.S.E.

The University of Texas at Austin, 2007

Supervisor: James O. Jirsa

Six beam specimens were tested with MMFX bars spliced in a constant moment region. Test variables included the use of transverse reinforcement and its spacing, and the number of spliced bars in the beam specimens. In all specimens, the bar size, concrete strength, splice length and the bar cover was held constant. Splice confinement was varied using transverse reinforcement

The splice lengths were instrumented with strain gauges to monitor bar stress distribution along the splice length. Four of the beam specimens included two spliced bars, with two of those specimens part of a collaborative test program mandating strain gauges on splice ends only. The remaining two specimens had three spliced bars to compare the behavior of the interior splice to that of the exterior splice. The interior

splice was thought to be confined less than the exterior splice; however no difference in behavior was noted.

Test results were compared with computed values using current development length equations. Stress variation along bars was linear. More splice confinement provided increased splice capacity. At high working stress levels (80-100 ksi) crack widths exceeded code serviceability requirements for Grade 60 reinforcement. No difference was noted in splice behavior when the splice length was gauged compared to the splice ends gauged only.

Table of Contents

List of Tables

List of Figures

Chapter 1: Background and Introduction

1.1 BACKGROUND

Microcomposite, multistructural, formable steel (MMFX) was designed as a corrosion resistant steel and has the added benefit of high strength. The reinforcing bar is not coated but is structured differently than conventional rebar at the atomic level to prevent corrosion. MMFX steel costs more than conventional rebar because of its new technology. However it may be economical if its high strength could be utilized at stresses higher than the ACI Building Code[1] limit of 80 ksi. One issue with high strength steel is bond and anchorage. The purpose of this study is to test MMFX reinforcing bars splices to study bar development at high stresses.

Currently there is very little information about bond of high strength steel. The ACI 408[2] database has a lot of bond and development test data, but almost all is for Grade 60 steel. A series of pullout tests were conducted at Michigan Tech University to determine whether the required development length for MMFX steel was equal to that required of A615 Grade 60 steel[3]. At North Carolina State University, beam-end pullout tests were also conducted[4]. Both studies concluded that bond behavior of MMFX steel is similar to that of Grade 60 steel. At the University of North Florida, beams with continuous MMFX tension steel were tested to determine if MMFX steel behaved in a ductile manner in flexure, comparable to Grade 60 steel[5]. The MMFX steel was found to be ductile, comparable to Grade 60. The test program at NC State also included beam-splice specimens. Bond capacity of the splices computed using code provisions and other published equations were less than test values for MMFX bars up to the code limit of 80 ksi. Thompson et al.[6] tested wide sections with multiple lap splices of conventional

Grade 60 steel and found that exterior splices or splices not confined by corners of the transverse reinforcement were weaker than interior splices.

1.2 COMPARISON OF EQUATIONS FOR DEVELOPMENT LENGTH

Current equations used to calculate splice development length are given in ACI 408R-03 and ACI 318-05.

1.2.1 ACI 408

ACI 408R-03 Equation (4-11a) was used to determine splice lengths. A description of the equation follows.

$$\frac{l_d}{d_b} = \frac{\left(\dfrac{f_y}{\phi \cdot f_c'^{1/4}} - 2400 \cdot \omega\right) \cdot \alpha \cdot \beta \cdot \lambda}{76.3\left(\dfrac{c \cdot \omega + K_{tr}}{d_b}\right)} \qquad \text{(Eq. 1-1)}$$

Where,

l_d = development or splice length

d_b = diameter of bar being developed or spliced

f_y = yield strength of steel being developed or spliced

f_c' = concrete compressive strength based on 6 x 12 in. cylinders

ϕ = capacity-reduction factor, with a value of 1.0 for mean results and a value of

    0.82 for lower fractile results

$\omega = 0.1\dfrac{c_{min}}{c_{max}} + 0.9 \leq 1.25$

c_{min} = minimum of c_b or c_s

c_{max} = maximum of c_b or c_s

c_b = bottom clear cover

c_s = minimum of c_{so} or c_{si}

c_{so} = side clear cover

c_{si} = one-half the bar clear spacing + 0.25 in.

α = reinforcement location factor

β = coating factor

λ = lightweight concrete factor

$c = c_{min} + 0.5\,d_b$

$$K_{tr} = \frac{0.52 \cdot t_r \cdot t_d \cdot A_{tr}}{s \cdot n} \cdot \sqrt{f_c'}$$

$t_r = 9.6R_r + 0.28 \leq 1.72$

R_r = relative rib area

$t_d = 0.78d_b + 0.22$

A_{tr} = area of each stirrup or tie crossing the potential plane of splitting adjacent to the reinforcement being developed, spliced, or anchored

s = spacing of transverse reinforcement

n = number of bars being developed or spliced

And $\dfrac{c \cdot \omega + K_{tr}}{d_b} \leq 4.0$ to prevent a pullout failure.

The splitting plane can propagate through the edge cover causing the clear cover to spall off, called *side splitting*, as shown in Figure 1.1(a) for a two splice specimen and (c) for a three splice specimen. Another splitting plane can propagate through the clear cover, called *face splitting*, as shown in (b) for a two splice specimen and (d) for a three splice specimen. A combination of side splitting and face splitting typically occurs, called *face-and-side-splitting*. Splitting plane terminology is consistent with that used in Orangun, Jirsa, Breen[7]. For the possible splitting plane shown in Figure 1.1(a), the splitting plane crosses the transverse reinforcement twice therefore $A_{tr} = 2 \cdot A_{tie}$, and the splitting plane crosses two splices therefore n = 2.
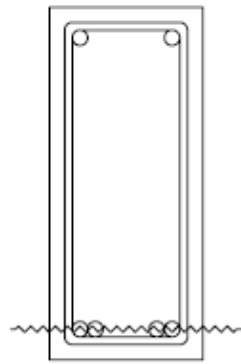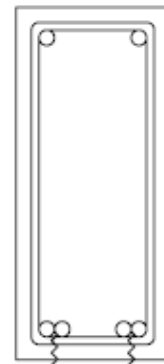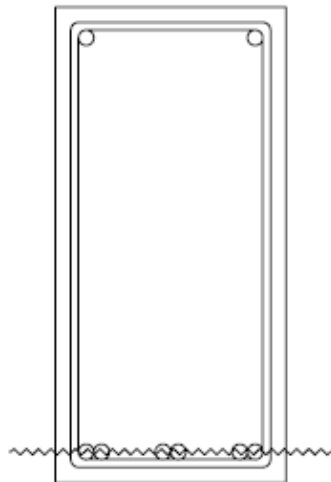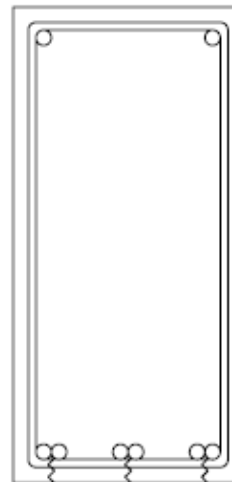
Figure 1.1: Potential Planes of Splitting for Two Splice and Three Splice Specimens and the Corresponding Atr and n values

1.2.2 ACI 318

The development length equation typically used by designers is equation (12-1) of ACI 318-05, which is based on the expression developed by Orangun, Jirsa, and Breen[7] and previously endorsed by Committee 408.

$$l_d = (\frac{3}{40} \cdot \frac{f_y}{\sqrt{f'_c}} \cdot \frac{\psi_t \cdot \psi_e \cdot \psi_s \cdot \lambda}{(\frac{c_b + K_{tr}}{d_b})}) \cdot d_b \qquad \text{(Eq. 1-2)}$$

Where,

ψ_t = reinforcement location factor

ψ_e = reinforcement coating factor

ψ_s = reinforcement bar size factor

λ = lightweight concrete factor

c_b = smaller of (a) distance from center of bar or wire to nearest concrete surface,

and (b) ½ the center-to-center spacing of bars or wires being developed

$$K_{tr} = \frac{A_{tr} \cdot f_{yt}}{1500 \cdot s \cdot n}$$

f_{yt} = yield strength of transverse reinforcement

And $\frac{c_b + K_{tr}}{d_b} \le 2.5$ to prevent a pullout failure.

1.2.3 Differences in Equations for Development Length

Several differences arise when comparing the two equations. A discussion of the most significant differences follows. To account for the effect of concrete compressive strength on bond strength, the ACI 408 equation (Eq. 1-1) specifies $f'_c{}^{1/4}$ while the ACI 318 equation (Eq. 1-2) uses $f'_c{}^{1/2}$. The calculation of the K_{tr} term in the ACI 408 equation is a function of f'_c, but in the ACI 318 equation K_{tr} does not consider f'_c, resulting in the

ACI 318 equation producing a higher K_{tr} value, and therefore a lower l_d, at lower values of f'_c. The limit to prevent a pullout failure is much higher in the ACI 408 equation. The method of calculating the limit is slightly different in each equation: the ACI 408 equation uses the smaller of bottom cover and side cover times a ratio taking into account the difference between the two covers, and the ACI 318 equation simply employs the minimum cover or spacing. More importantly, the limit placed on the ACI 408 equation is 4.0 while the limit placed on the ACI 318 equation is 2.5. It should be pointed out that ACI 318 is thought of as a lower fractile equation, and is not a mean value equation directly comparable with $\Phi=1.0$ in the ACI 408 expression.

1.3 INTRODUCTION

To provide data on bond of high strength reinforcement, a collaborative test program was developed and a series of tests were conducted at The University of Texas at Austin, NC State University, and The University of Kansas. Guidelines were set for the test procedure. Beams with two spliced MMFX reinforcing bars (No. 5, 8, or 11) were tested. Concrete strengths of 5 ksi and 8 ksi were specified. Bar cover ranged from ¾ in to 3 in. Splice lengths and splice confinement varied. To measure strains, strain gauges were attached at the splice ends. No gauges were attached along the splice to ensure that bond behavior along the splice was not compromised.

The objective of the test program summarized in this report was to extend the range of the collaborative test program by further varying the splice confinement and the number of spliced bars. Four specimens were constructed. Two of the specimens were duplicates of the specimens that were part of the collaborative test program but the entire splice length was gauged for comparison with the companion tests. The other two specimens contained three spliced bars and the confinement provided by transverse reinforcement around the lap splice was varied.

6

Chapter 2: Test Program

2.1 DESCRIPTION OF SPECIMENS

All test specimens were beams with two or three lap spliced tension MMFX reinforcing bars at midspan. Other properties were held constant in all specimens. No. 8 bars were used, a 1.5 in. cover was maintained around each tension bar, the splice length was 40 in., concrete compressive strength was approximately 8 ksi, Grade 60 compression steel was used, and No. 4 Grade 60 closed ties were used outside of the splice region as shear reinforcement. Four of the six specimens also had these ties in the splice region.

To avoid lower bond strengths associated with top bar effects, the beams were cast with the MMFX tension bars at the bottom of the section and rotated before testing so that the MMFX tension bars were at the top of the beam.

During testing, the splice was under uniform stress in a constant moment region. This was achieved with a two-point loading system.

2.2 SPECIMEN DETAILS AND VARIABLES

Beam dimensions were calculated based on given cover and bar spacings determined in the collaborative test program. All beams were designed such that the concrete should reach crushing strains when the MMFX steel reached a stress of 150 ksi. The stress-strain relationship of the MMFX steel used in the designs was determined from tension tests. Concrete stress-strain relationships were idealized using the Whitney stress block and an ultimate strain of 0.003.

Compression steel was included to reduce the amount of concrete needed to develop the compression zone and therefore the required height of the beams. The

amount of compression reinforcement was chosen to produce reasonably sized cross-sections. All compression steel is Grade 60.

Transverse reinforcement was included outside of the test region in all specimens to prevent shear failure. Number 4 Grade 60 ties were used as indicated in Table 2.1.

(Eq. 1-1) with Φ=1.0 was used to determine splice lengths. In the calculations, a nominal value of relative rib area (R_r) was used. Although the relative rib area of MMFX bars is reported to be greater than that of conventional reinforcing bars, which is 0.0727, actual MMFX values were not known at the time of specimen design. The relative relative rib area was assumed to be 0.075 for design, resulting in t_r = 1.0. Small changes in the value of R_r had practically no effect on calculated capacities. The K_{tr} term was first assumed to be zero, which means no transverse reinforcement in the splice region, for calculating the splice length. Then the K_{tr} term was varied for different confinement levels of the splice in order to reach a predetermined stress value in the MMFX bar. For higher levels of bar stress, Number 4 Grade 60 ties were used in the test region of all specimens with $K_{tr} > 0$. The designs include values of K_{tr} selected so that stress levels of 80 ksi, 90 ksi, and 100 ksi were reached (OC0, OC1, and OC2 specimens respectively).

The splice lengths and confinement levels required to achieve the desired stresses in the MMFX reinforcement are specified in Table 2.1. A confinement level of zero, C0, means no confinement of the splice. A confinement level of one, C1, means light confinement of the splice. Finally, a confinement level of two, C2, means heavy confinement of the splice. The light and heavy confinement terms are relative to each other for a certain specimen size.

The terminology used for the test names is consistent with that of the collaborative test program and is described in Figure 2.1. The cross sections of the two

8

splice and three splice specimens are shown in Figure 2.2. Details of all tests are described in Table 2.1.

8-8-2-OC0

Splice Confinement
(C0: No confinement
C1: Light confinement
C2: Heavy confinement)

Bar Stress
(O: 80, 90, 100 ksi
X: 100, 110, 120 ksi)

No. of Splices
(2 or 3)

Concrete Strength
(5, 8 ksi)

Bar Size
(#5,#8,#11)
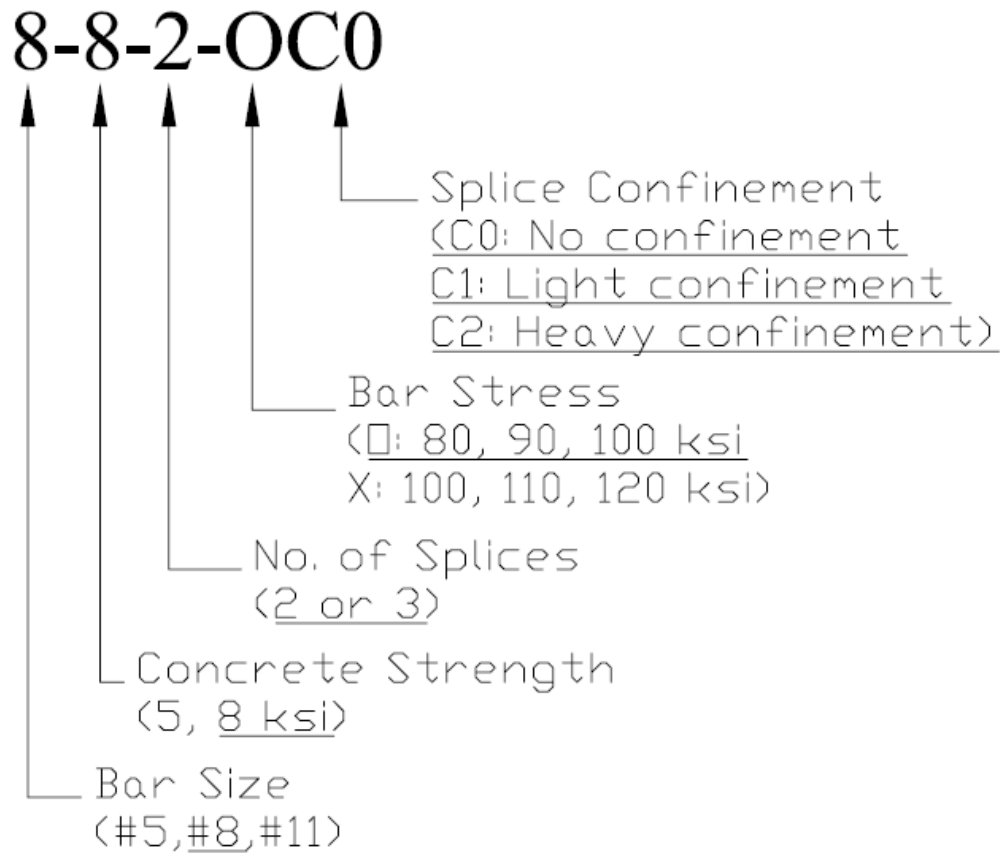
Note: Only underlined parameters used in this test program

Figure 2.1: Explanation of Test Terminology
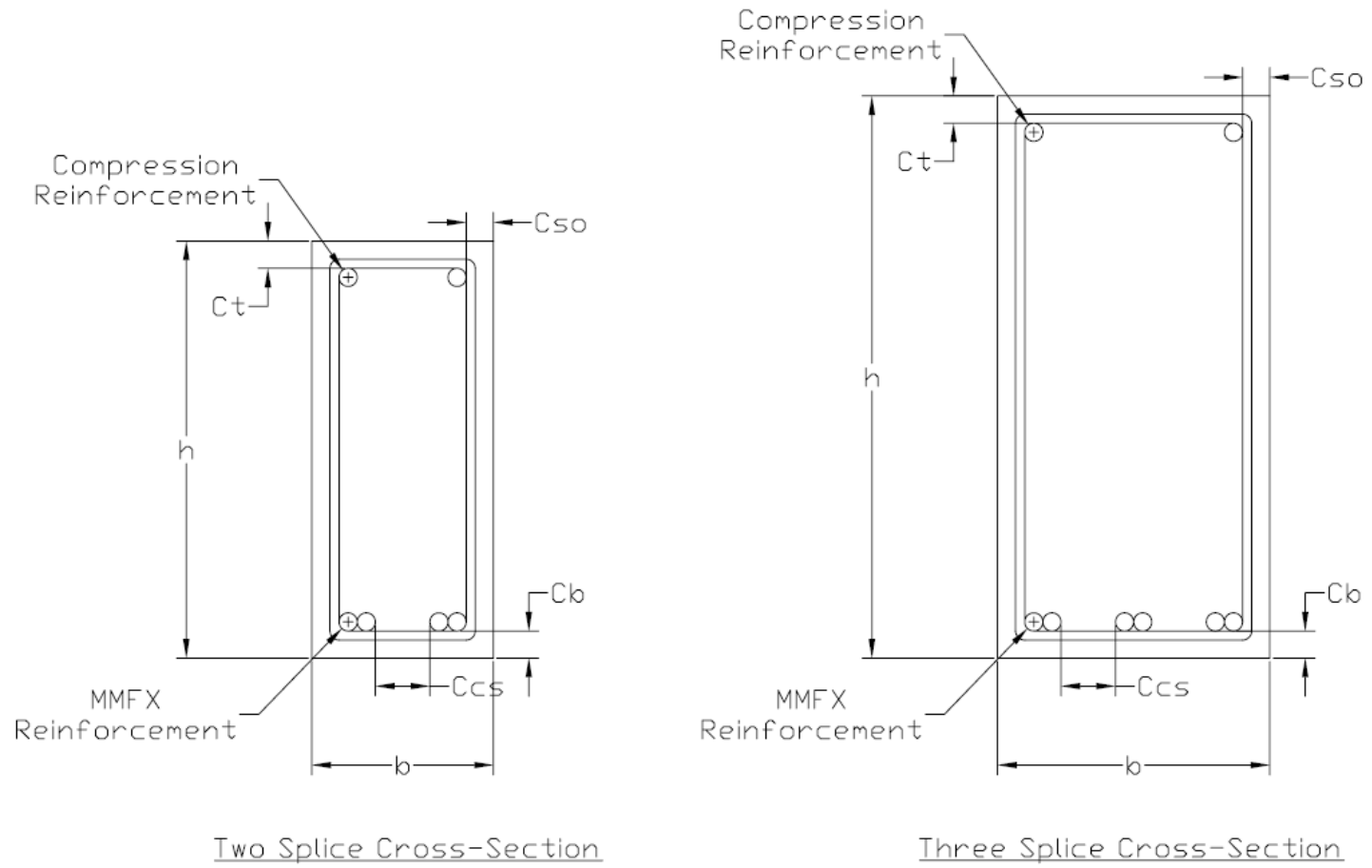
Figure 2.2: Typical Cross Sections

Test Name	No. Splices[+]	Strain Gauges on Splice	f'c (ksi)	Splice Confinement, No. 4 tie spacing (in)	b (in)	h (in)	c_{cs} (in)	c_{so} (in)	c_t (in)	c_b (in)
8-8-OC0*	2	ends only	8.3	N/A	10-1/4	22-3/8	2.8	1.6	3	1.5
8-8-OC1*	2	ends only	8.3	13-1/2	10-1/8	23-1/4	2.75	1.65	3	1.5
8-8-2-OC0	2	full length	7.9	N/A	10-1/8	23	3	1.5	2	1.5
8-8-2-OC1	2	full length	7.9	13-1/2	10-1/4	23-1/4	3	1.5	2	1.5
8-8-3-OC1	3	full length	8.5	13-1/2	15-1/8	31-1/4	3	1.5	2	1.5
8-8-3-OC2	3	full length	8.5	7	15-1/4	31-1/4	3	1.5	2	1.5

* Part of collaborative test program

[+]All splice lengths 40"

Table 2.1: Specimen Descriptions

2.3 MATERIALS

2.3.1 Concrete

Ready-mix concrete from a local supplier was used to cast all specimens. Type 1 cement, sand and 1 in. gravel was used. The water-to-cement ratio was reported as 0.44. The slump was measured from the truck to be between 6 and 8 in. for all specimens. The design minimum compressive strength was 7000 psi. The actual compressive strengths for each test are shown in Table 2.1 and ranged from 7900 to 8500 psi.

2.3.2 Steel

2.3.2.1 MMFX Reinforcement

Tension tests were conducted on No. 8 MMFX bars provided by the MMFX Corporation. The bars were tested in a 600 kip capacity testing machine, and elongation was measured using an 8 in. gauge length extensometer. Only two tests were conducted on the No. 8 bars because they displayed consistent behavior from the first bar test to the second bar test.

The exponential curve fit was developed using the data of the No. 8 bars. The exponential relationship is:

$$f_{MMFX} = 156 \cdot (1 - e^{-220 \cdot \varepsilon})$$

The test data and best curve fit are plotted in Figure 2.3.

MMFX #8 Stress-Strain
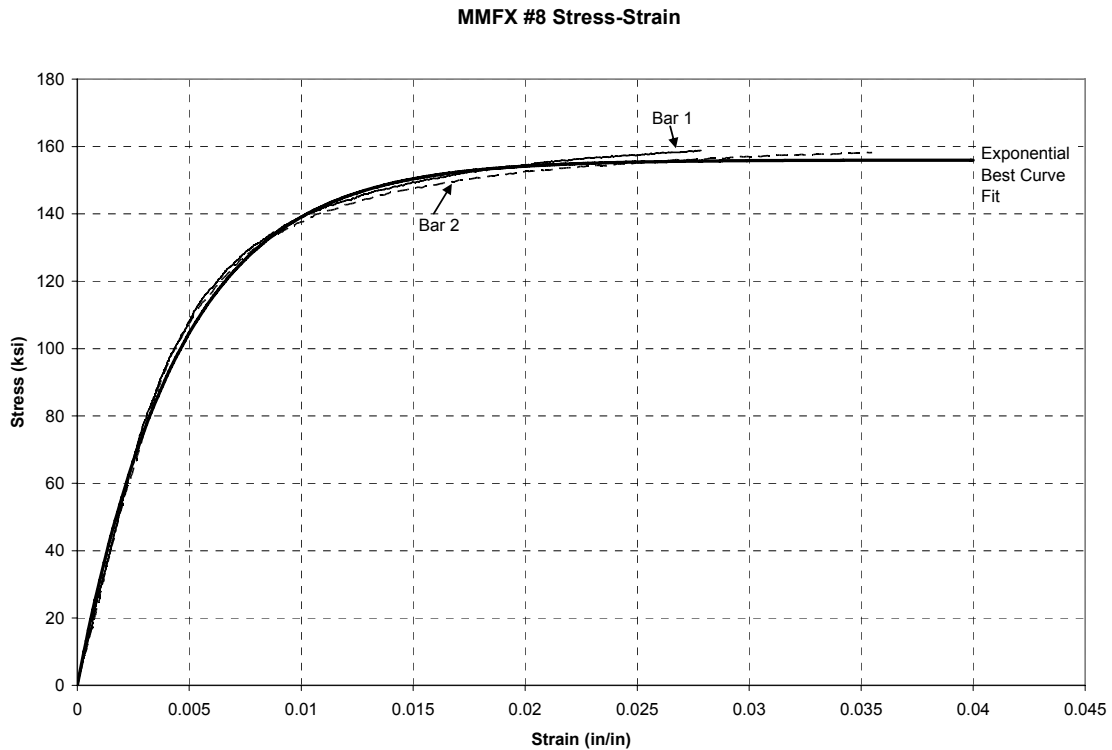
Figure 2.3: Stress-Strain Relationship for MMFX No. 8 Bars

2.3.2.2 Grade 60

All compression and transverse reinforcement was Grade 60. There were no tests run in the lab.

2.4 FABRICATION OF SPECIMENS

The MMFX tension reinforcement was cut to length. The 40 in. splice length was measured and marked on each bar. Before the cages were constructed, the bars were instrumented with four strain gauges placed along each splice at 10 in. spacings. A small section of the rebar rib or lug was ground off to create a smooth, flat surface for the strain gauge. The bar was then cleaned and the strain gauge was glued on, followed by an application of sealant. A thin rubber pad was placed on top of the dried sealant to protect

13

the gauge, and foil tape was tightly wrapped around the entire bar. Electrical tape was then tightly wrapped around the foil tape edges to seal the strain gauge site. The foil and tape were pressed firmly around the rebar lugs. The finished strain gauge site was approximately a 2 in. section covered by tape around the bar. There was concern that for tests in the collaborative test program, gauging would destroy too much surface area and affect bond behavior so no gauges were applied along the splice. A photograph of the strain gauged site on a completed rebar cage is shown in Figure 2.4.
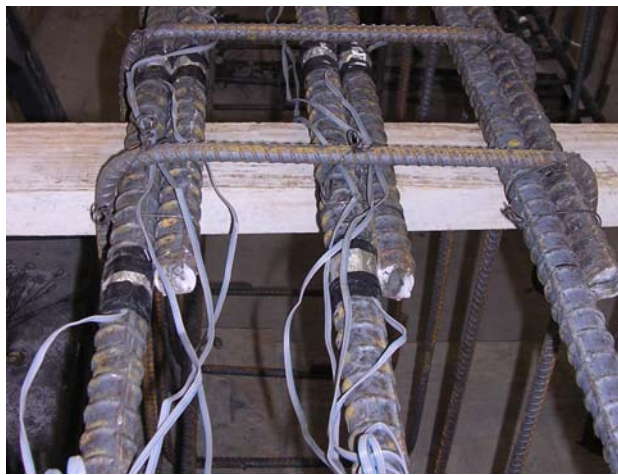
Figure 2.4: Finished Strain Gauge Site

A schematic showing gauge placement on spliced bars can be seen in Figure 2.5. In the two splice specimen, both splices were instrumented. In the three splice specimen, one exterior splice and the interior splice were instrumented. For the two splice specimens that were part of the collaborative test program, only gauge 4 at the splice end was applied to all bars. Photographs of the gauged splice region of both the two splice specimens and the three splice specimens are shown in Figure 2.6.

14
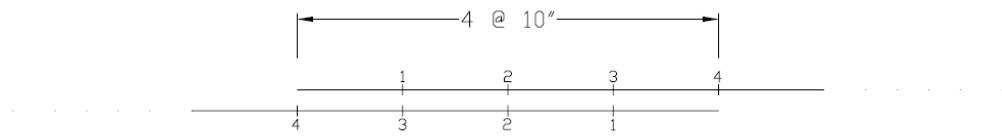
Figure 2.5: Gauge Placement on Splices
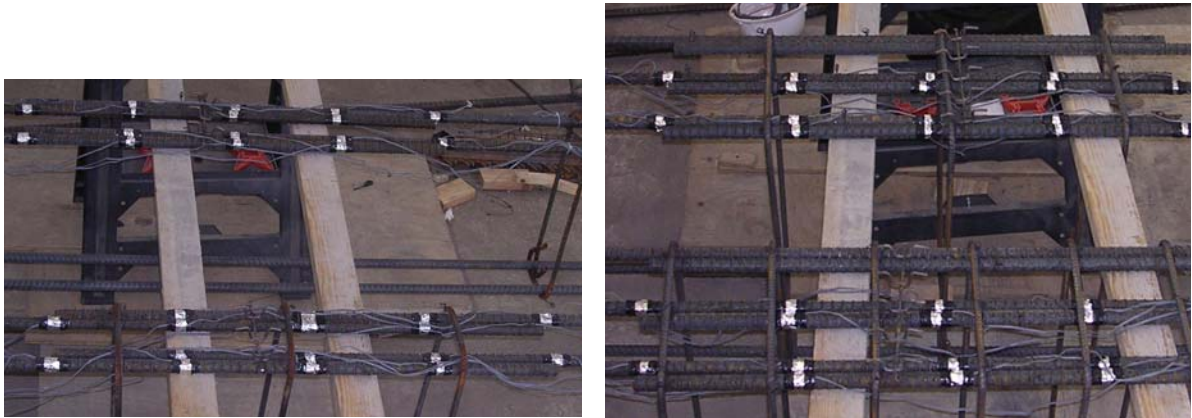
(a) Two Splice Specimens

(b) Three Splice Specimens

Figure 2.6: Photos of Splice Regions Showing Gauge Placement

After gauge application, spliced bars were held in place with tie wires to create a 40 in. splice. Transverse reinforcement was carefully placed and tied, first in the test region if necessary, and then in the shear region. For all tests, transverse reinforcement was provided in the 5 ft shear span between the load and end support to prevent shear failure before flexural or splice failure occurred.

Next the compression reinforcement was inserted through the stirrups and tied. All compression reinforcement was No. 8 bars (Grade 60) cut to length. Compression reinforcement was used so less concrete was needed to develop the compression force in the section. Also, the compression reinforcement helped hold the transverse reinforcement in place when the cages were later rotated and set into the formwork.

15

Four lifting inserts were secured to the rebar cages, two on top and two on bottom to facilitate lifting and rotating of the cured specimens with an overhead crane. Chairs were attached to the bottom and sides of the cages to ensure the specified concrete cover. Fabricated rebar cages before placement in forms are shown in Figure 2.7.

Figure 2.7: Fabricated Rebar Cages

At this stage of construction, gauges were on the bottom of the bars to prevent damage from mechanical vibrators during concrete placement. Formwork sides and bottom were constructed of plywood sheets and 2 x 4 boards. The forms were heavily braced along the sides to maintain specimen dimensions when subjected to the pressures of fluid concrete. The cages were lifted by crane, rotated 180°, and set into wooden formwork. Photos of the rebar cages placed in the formwork for the two splice and three splice specimens can be seen in Figure 2.8.

(a) Two Splice Specimens   (b) Three Splice Specimens

Figure 2.8: Rebar Cages Set in Formwork

Specimens were cast using ready-mix concrete. The slump was checked and water was added if necessary before the concrete was placed. Concrete was placed in three lifts using a bucket on a crane. See Figure 2.9. After each lift, the concrete was vibrated with a mechanical vibrator. To ensure quality control, 6 in. x 12 in. cylinders were also cast and used to measure the concrete strength throughout the curing process. The concrete surface was screeded and then troweled, as shown in Figure 2.10, to produce a smooth finish. See Figure 2.11.

(a) Slump Test

(b) Use of Bucket

Figure 2.9: Concrete Placement

(a) Vibrating Concrete

(b) Screeding Concrete Surface

Figure 2.10: Consolidation and Finishing

(a) Two Splice Specimens   (b) Three Splice Specimens

Figure 2.11: Finished Specimens

After the concrete was placed, the specimens and cylinders were covered with a polyethylene sheet for a minimum of twenty four hours to prevent shrinkage cracking. The cylinders were cured next to the specimens in the laboratory.

When the concrete had reached sufficient strength, an overhead crane was used to remove the specimens from the formwork, and they were placed on the lab floor to reach their specified concrete compressive strength. When the desired concrete strength was achieved, the specimens were lifted by overhead crane and rotated 180° so the spliced bars would be on the top face (the tension face) of the beam during testing. The locations

of the splice ends were marked on the beams so location of cracks relative to splice position could be easily observed during testing. The two desired locations for ram loading were marked on the beam to ensure the splice would remain in a constant moment region. The specimens were then lifted by crane and placed into the test set-up and centered above the rams that were in place on the lab floor. Strain gauge wires were checked and connected to the data acquisition system. Final beam dimensions were measured and recorded.

2.5 SPECIMEN LOADING SYSTEM

2.5.1 Constant Moment Loading System

All beams were simply supported on the ends with two identical point loads applied by two hydraulic rams acting in an upward direction in the center region of the span. This configuration was chosen to facilitate crack measurements and observation. A photo of the test set-up can be seen in Figure 2.12 and a schematic is shown in Figure 2.13. The span is 16 ft and the spacing of the loading rams is 6 ft. Spans were chosen in 4 ft increments to align with tie down points in the laboratory strong floor. Ram spacings were chosen to provide a constant moment region longer than the splice length, and beam lengths were selected such that the failure loads would be compatible with the laboratory equipment and test floor capacities.

Two large concrete blocks were used in the set-up to support the beam prior to testing. The blocks also served as a safety system should beam failure cause the beam to fall.

A roller with a plate was placed under each reaction beam to create a simply supported boundary condition. The load was transferred from the rams, through the beams, through the rollers to the reaction beams. From the reaction beams, the load was

transferred through tie down rods to the lab strong floor. The tie down rods were very flexible and did not provide any longitudinal restraint to the specimens.

Two rams were connected to the same manifold to maintain constant pressure at the rams. A load cell was placed under each ram to monitor the applied load, and a pressure transducer was placed in the hydraulic line.

Figure 2.12: Photo of Test Set-up

Stirrup Schedule	
Test Name	Stirrups, No.4 @ (in)
8-8-□C0	9.5
8-8-□C1	9.5
8-8-2-□C0	9.5
8-8-2-□C1	9.5
8-8-3-□C1	5
8-8-3-□C2	5

Figure 2.13: Schematic of Test Set-up

2.5.2 Dead Loadings on the Specimen

Prior to testing, the concrete beam was resting on two large concrete blocks in the test set-up. To initiate testing, the rams were slowly lifted causing the rollers, which were placed on the test specimen, to make contact with the reaction frame. Once the initial
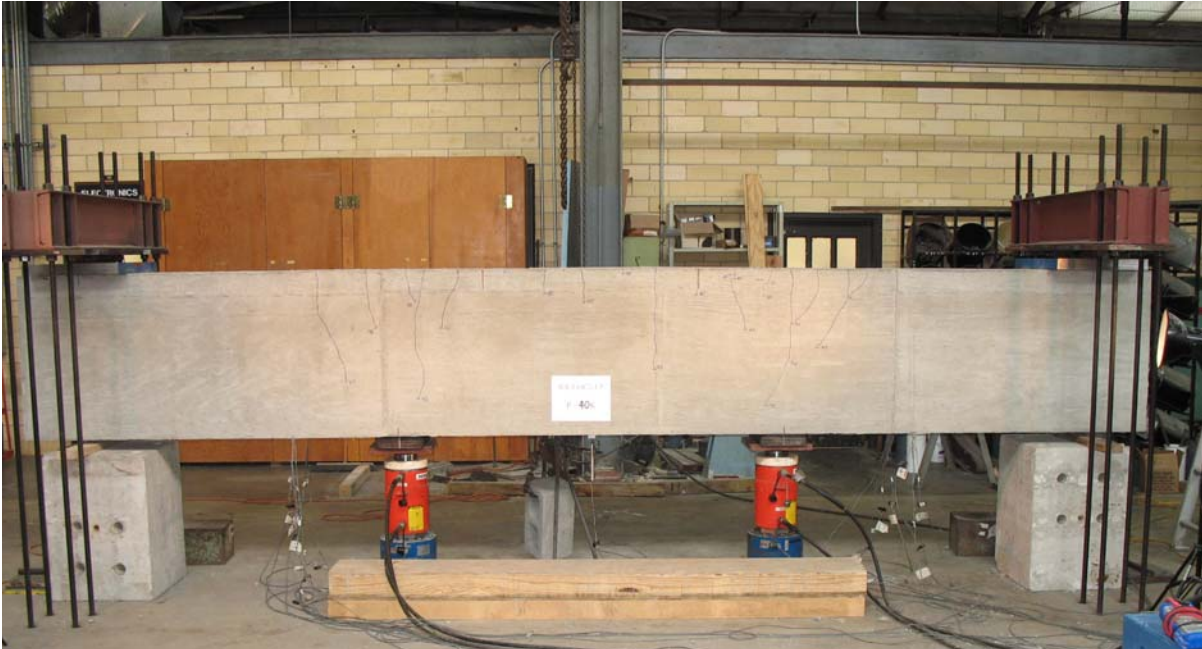
contact was made between the beam and the reaction frame, the ram load readings were zeroed out in the data acquisition system to exclude the weight of the beam in the applied ram load readings.

2.6 TEST PROCEDURE

A data acquisition system was used to monitor the different instruments. A load cell under each ram measured the force applied to the beam. A pressure transducer in the hydraulic line measured the pressure to the rams. Strain gauges in the splice region measured variations in the MMFX bar strains. A deflection transducer measured the beam deflection at midspan. The computer monitor displayed force applied to the beam as load cell readings and strain gauge readings, which were used to monitor the rate at which load was applied and to control load increments. Load was applied in increments of 5 to 10 Kips or smaller as the beam approached failure. The instruments continuously scanned during loading. The data acquisition system was not running at the end of each load step, when cracks were measured and photographs were taken. Crack width measurements were estimated using a crack comparator. Measurements were taken at each load step at the two splice ends and at the center of the splice. Cracks were marked and photos were taken to mark crack progression. An example of data acquisition output of a two splice test conducted as part of the collaborative test program is shown in Figure 2.14, which clearly shows the increments where the loading was stopped for measurements and observations.
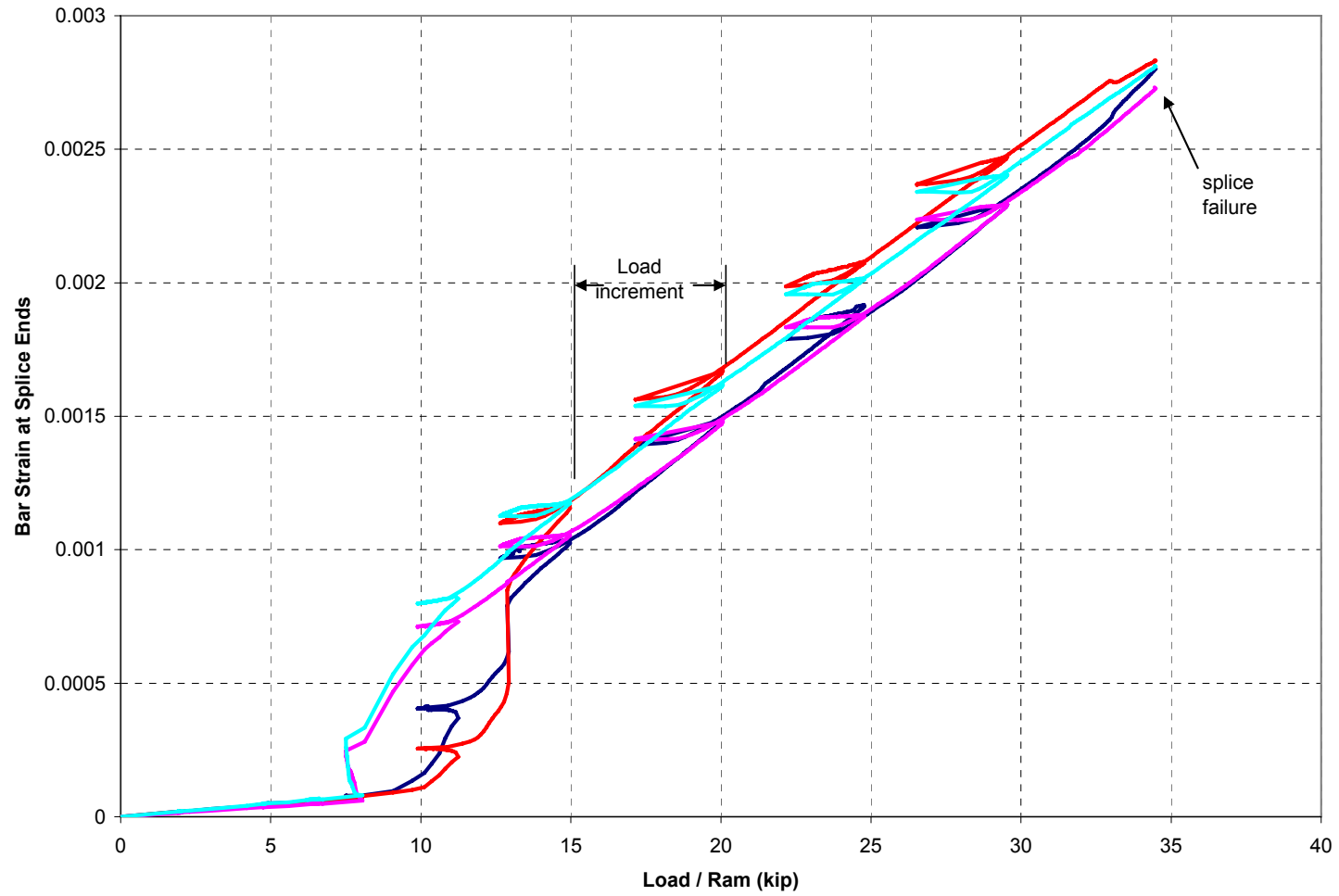
Figure 2.14: Example of Data Acquisition Monitoring, 8-8-OC0

Chapter 3: Test Results and Observations

3.1 FAILURE MODES

The failure modes in all tests were similar in that splitting of the concrete cover caused splice failure, which is shown in Figure 3.1. Initial splitting occurred in the cover of the edge bar, perpendicular to the splice, called *side splitting*. As load increased and bar stress increased, more load was transferred along the splice length and therefore cracks progressed in regular increments down the splice length, perpendicular to the splice. At high loads, cracks developed on top of the splice length, called *face splitting*. In tests without splice confinement, much more concrete spalled off compared to tests with splice confinement. The two splice specimens failed in a combination of face and side splitting. The three splice specimens failed in side splitting.
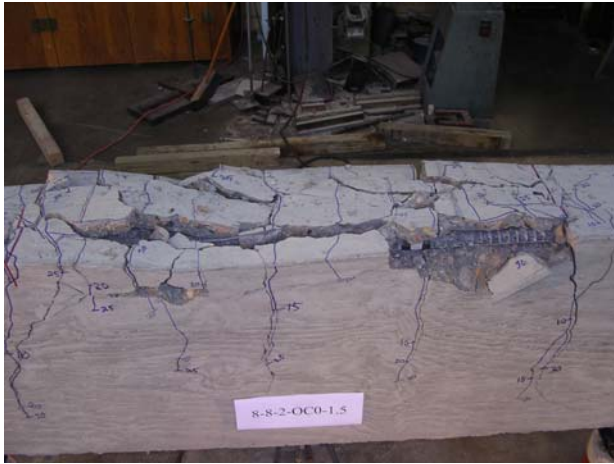
(a) 8-8-2-OC0: Face and Side Split Failure

(b) 8-8-2-OC1: Face and Side Split Failure

(c) 8-8-3-OC1: Side Split Failure

(d) 8-8-3-OC2: Side Split Failure

Figure 3.1: Appearance of Specimen after Failure

3.2 CRACK WIDTHS

The bar stress was highest at the splice ends, and therefore flexural cracks at splice ends formed first and were the widest cracks throughout the test. Crack widths at splice ends were measured using a crack comparator at each load step.

Crack width data is graphed in Figure 3.2 for the four specimens with the splice fully gauged: 8-8-2-OC0 (two splice specimen with no confinement), 8-8-2-OC1 (two splice specimen with light confinement), 8-8-3-OC1 (three splice specimen with light confinement), and 8-8-3-OC2 (three splice specimen with heavy confinement). Cracks at both ends of the splice are shown. Crack widths at midsplice were monitored but remained very small and did not progress as stress increased and are not included in the graph. ACI 318 historical crack width limits at service loads (approximately $0.6 f_y$) are included for reference.

Crack widths at splice ends did not increase linearly with bar stress but increased exponentially until failure occured.
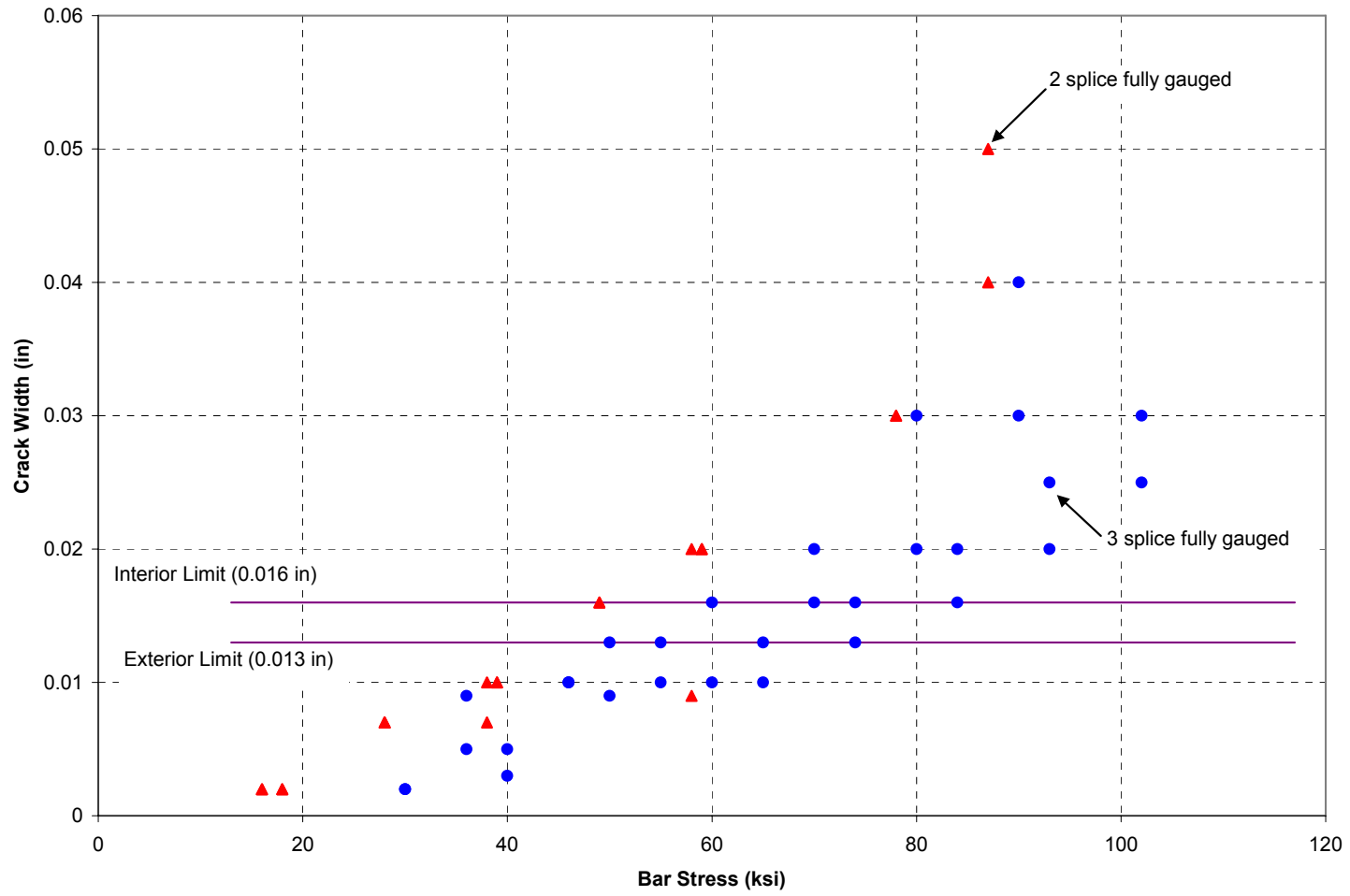
Figure 3.2: Crack Widths of Four Specimens with Fully Gauged Splice Lengths: 8-8-2-OC0, 8-8-2-OC1, 8-8-3-OC1, 8-8-3-OC2

3.3 BAR STRESS

The data from the data acquisition system was in terms of strain and force as shown in Figure 3.3. Irregularities in the plot that were obviously due to the interruptions of loading when the desired load increment was reached were smoothed out. Strain gauge readings were converted to stress using the stress-strain relationship for MMFX bars.

The ram load needed to produce a bar stress of 140 ksi was used to normalize the load for each specimen. For example, using (Eq. 1-1) for specimen 8-8-2-OC0 shown in the following figures, a calculated ram load of 70.97 kips would produce a bar stress of 140 ksi. A P/P_{140} ratio of 0.5 would indicate a ram load of 35.49 kips, which resulted in a bar stress of 73 ksi during testing of the specimen. See Figure 3.4.

Bar stress was then plotted along the splice length for various load ratios. This allowed the comparison of different tests in terms of load ratios. Stress readings for four bars were averaged into a single curve as seen in Figure 3.5. Similar procedures were used for all tests.
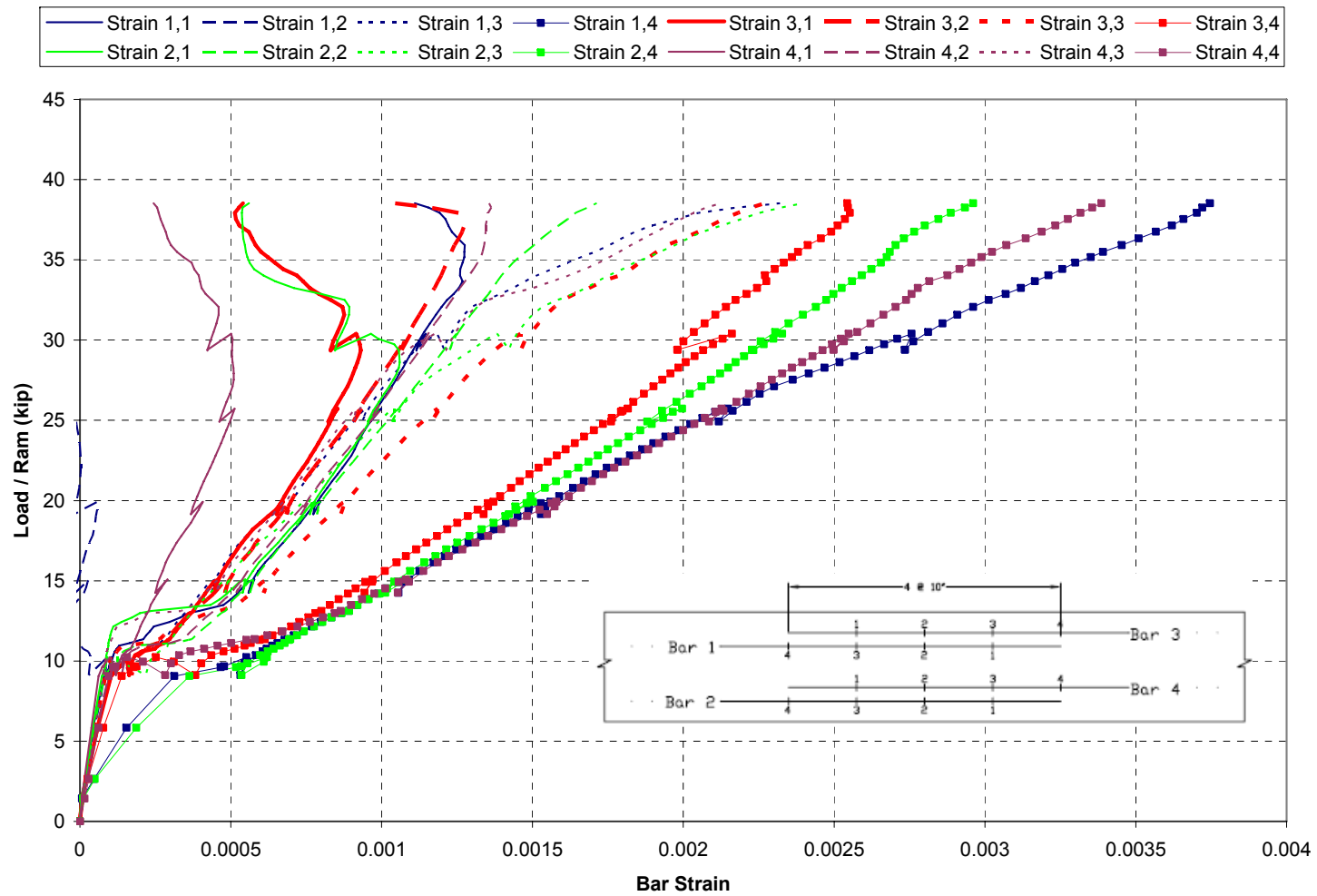
Figure 3.3: Specimen 8-8-2-OC0 (No Confinement), Typical Raw Test Data
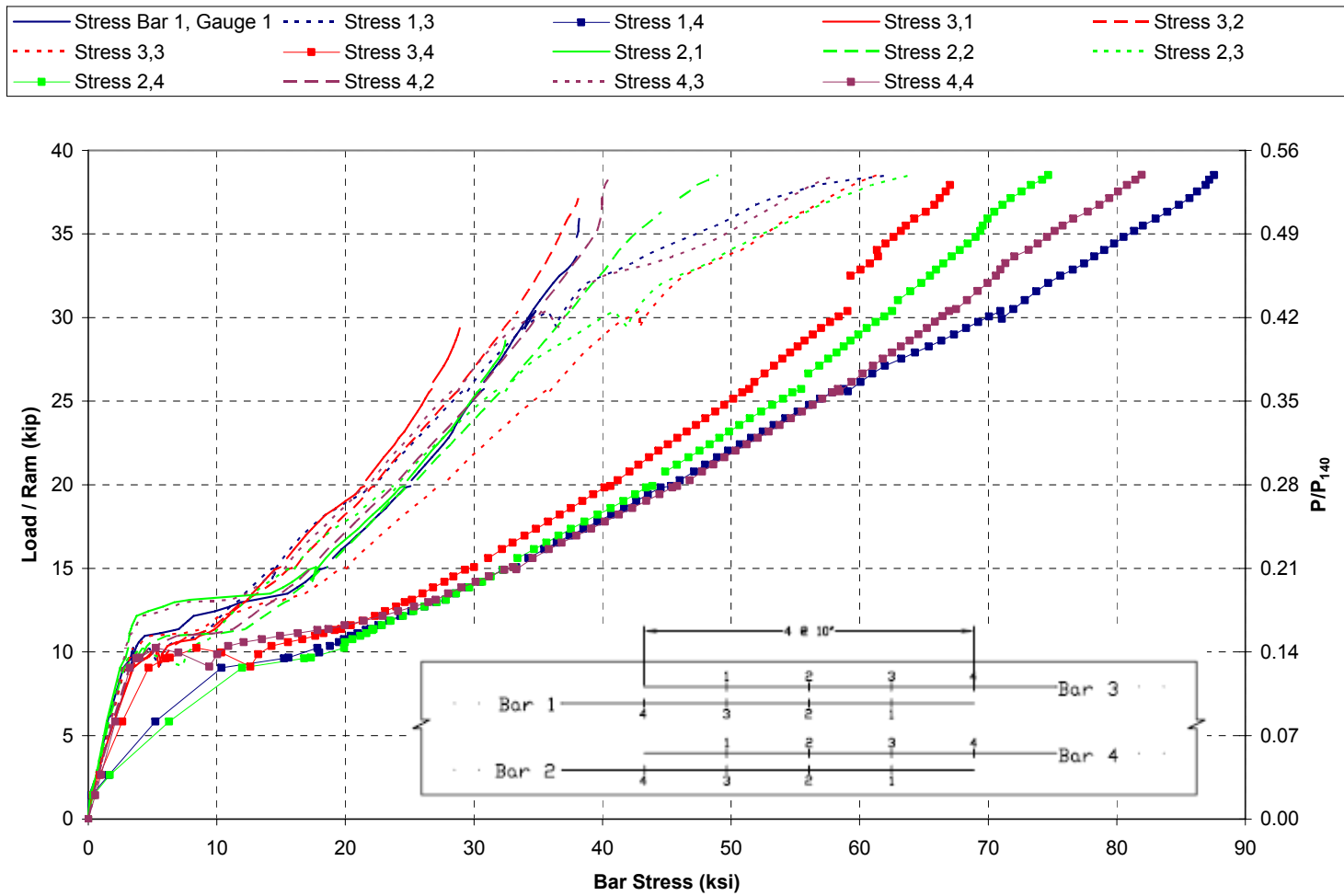
30

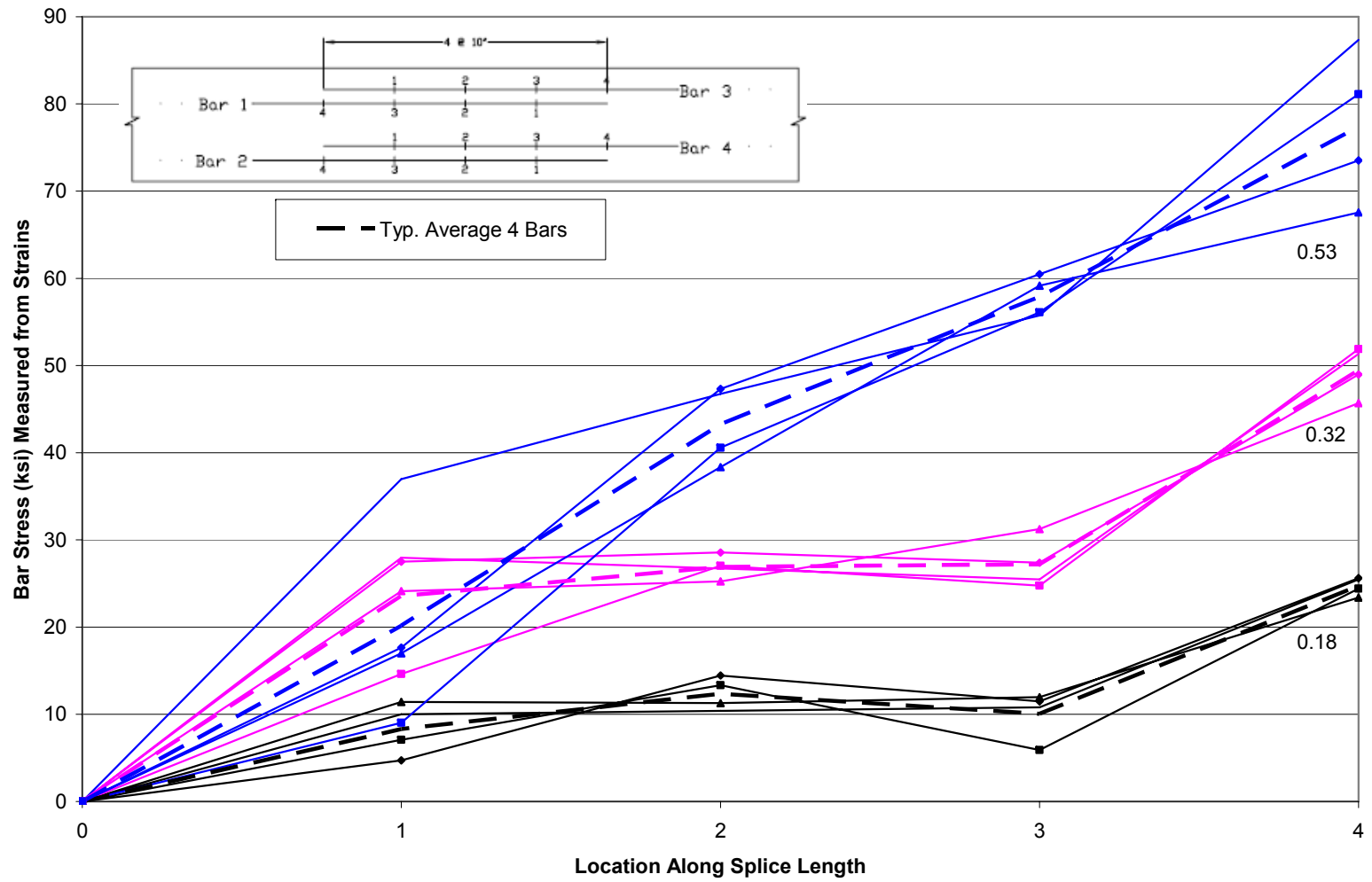Figure 3.4: Specimen 8-8-2-OC0 (No Confinement), Strain Data Converted to Stress, Addition of Load Ratio

31

Figure 3.5: Specimen 8-8-2-OC0 (No Confinement), Stress Along Splice at Various P/P$_{140}$ Ratios, Average of Four Bars

3.3.1 Two Splice Tests

The stress variation along the splice of the two splice specimen with no splice confinement is shown in Figure 3.6. The stress variation along the splice of the two splice specimen with light splice confinement (No. 4 stirrups spaced at 13.5 in) is shown in Figure 3.7.

Both specimens initially show higher stresses at the splice end, but the curve gradually becomes linear near failure. At low stress levels, the splice end is carrying much higher stress than at the splice midspan. This is probably due to the cracking patterns discussed earlier. A comparison of the two splice specimen bar stress along the splice with no confinement to bar stress along the splice with light confinement is shown in Figure 3.8. At comparable stress levels there is very little difference between the specimen without confinement and the specimen with light confinement. There is a greater difference between the two specimens at low stress levels. As the specimen reaches failure, this level of confinement does not appear to affect bar stress in the splice.
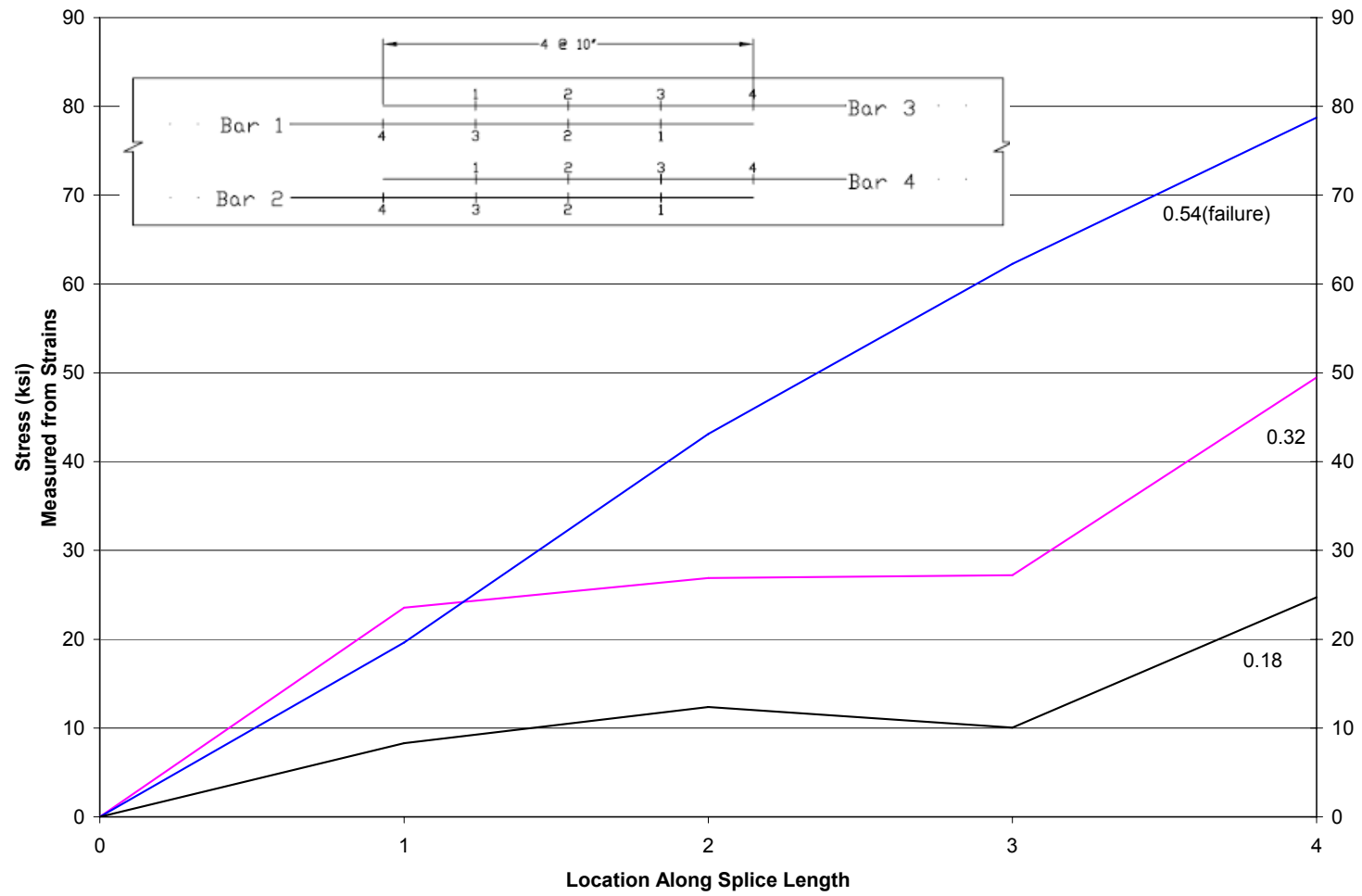
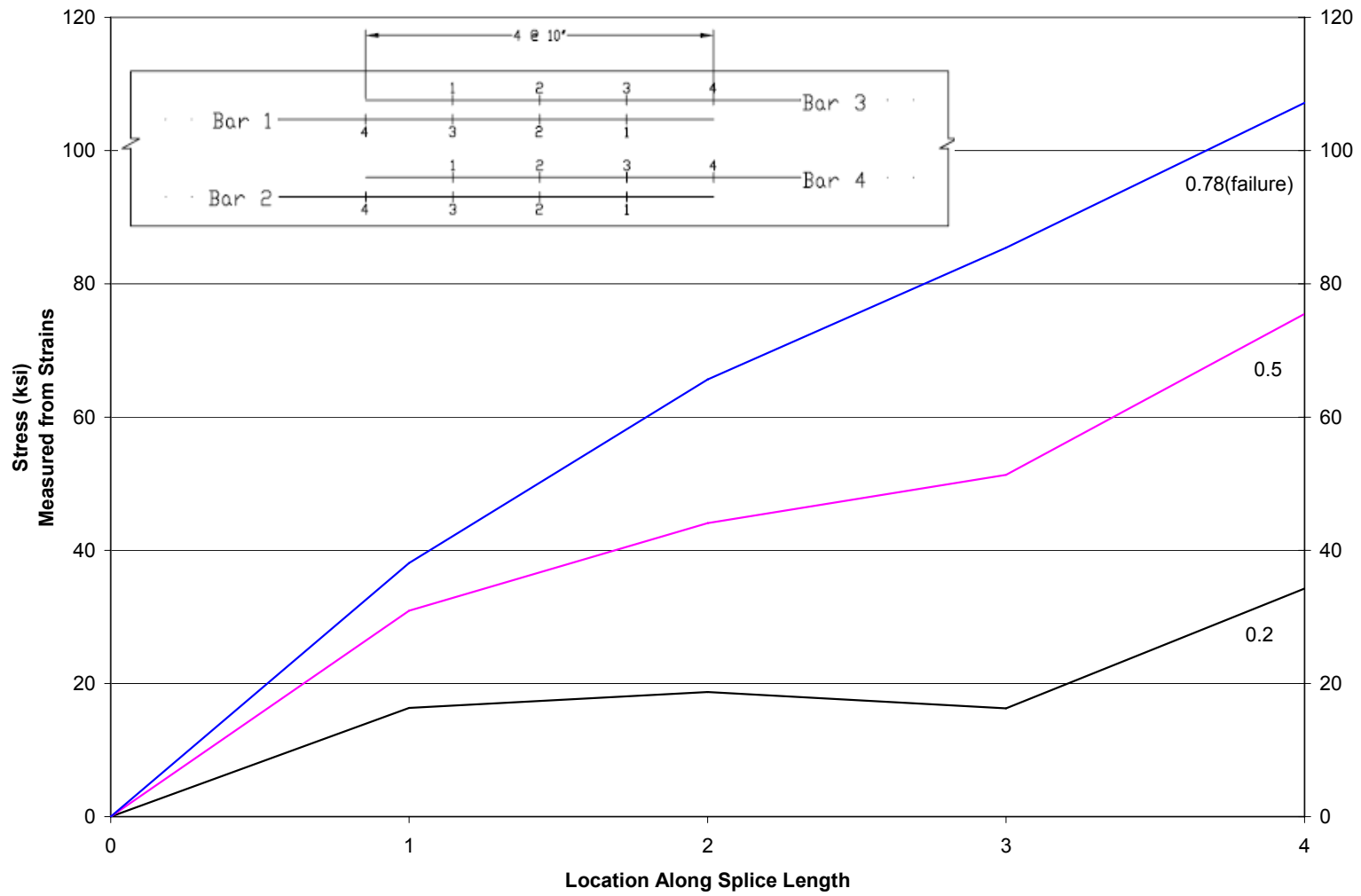Figure 3.6: Specimen 8-8-2-OC0 Bar Stress Along Splice (No Confinement)

Figure 3.7: Specimen 8-8-2-OC1 Bar Stress Along Splice (Light Confinement)
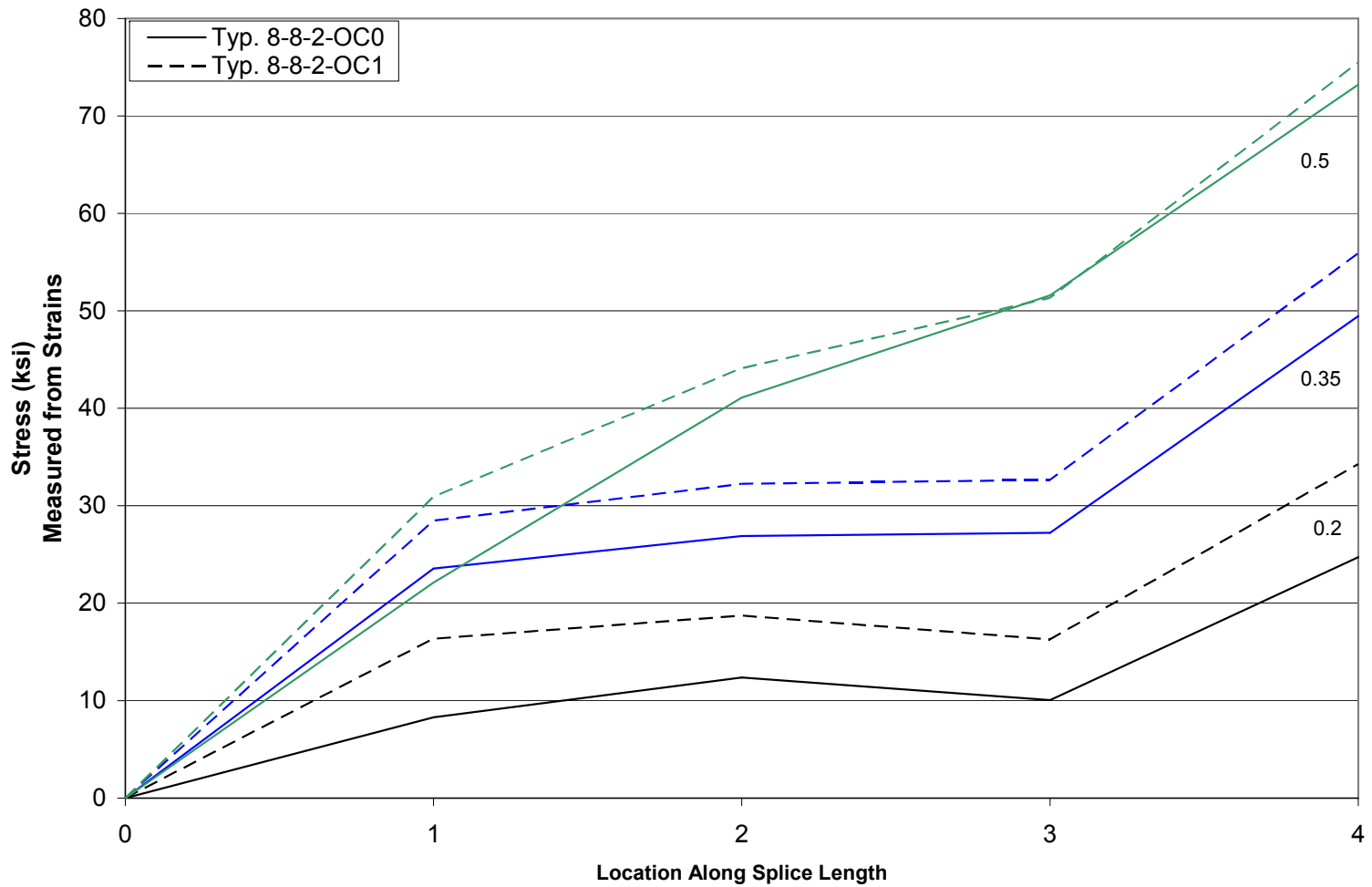
Figure 3.8: Comparison of Two Splice Specimens 8-8-2-OC0 (No Confinement) to 8-8-2-OC1 (Light Confinement) Bar Stress Along Splice

3.3.2 Effect of Strain Gauges Along Splice Length

A comparison of bar stress versus ram load for the two splice specimens with strain gauges at splice ends only (tested by Glass[8]) to the stresses with the splice length fully gauged provides an indication of any loss of strength due to the disruption of bond at the three additional strain gauge locations along the splice length. A comparison of the two splice specimens with no splice confinement is shown in Figure 3.9, and a comparison of specimens with light confinement is shown in Figure 3.10.

The additional gauges appear to have little or no effect on the bond behavior. This may be due to the fact that only one bar lug was ground off to attach the strain gauge. Since the force required to split the concrete cover is the same regardless of the number of lugs acting against the cover along the 40 in. splice, the loss of a small protrusion of the contact area between the bar and the concrete did not alter bond behavior. The loss of contact may be more pronounced in cases where pullout failure occurs.

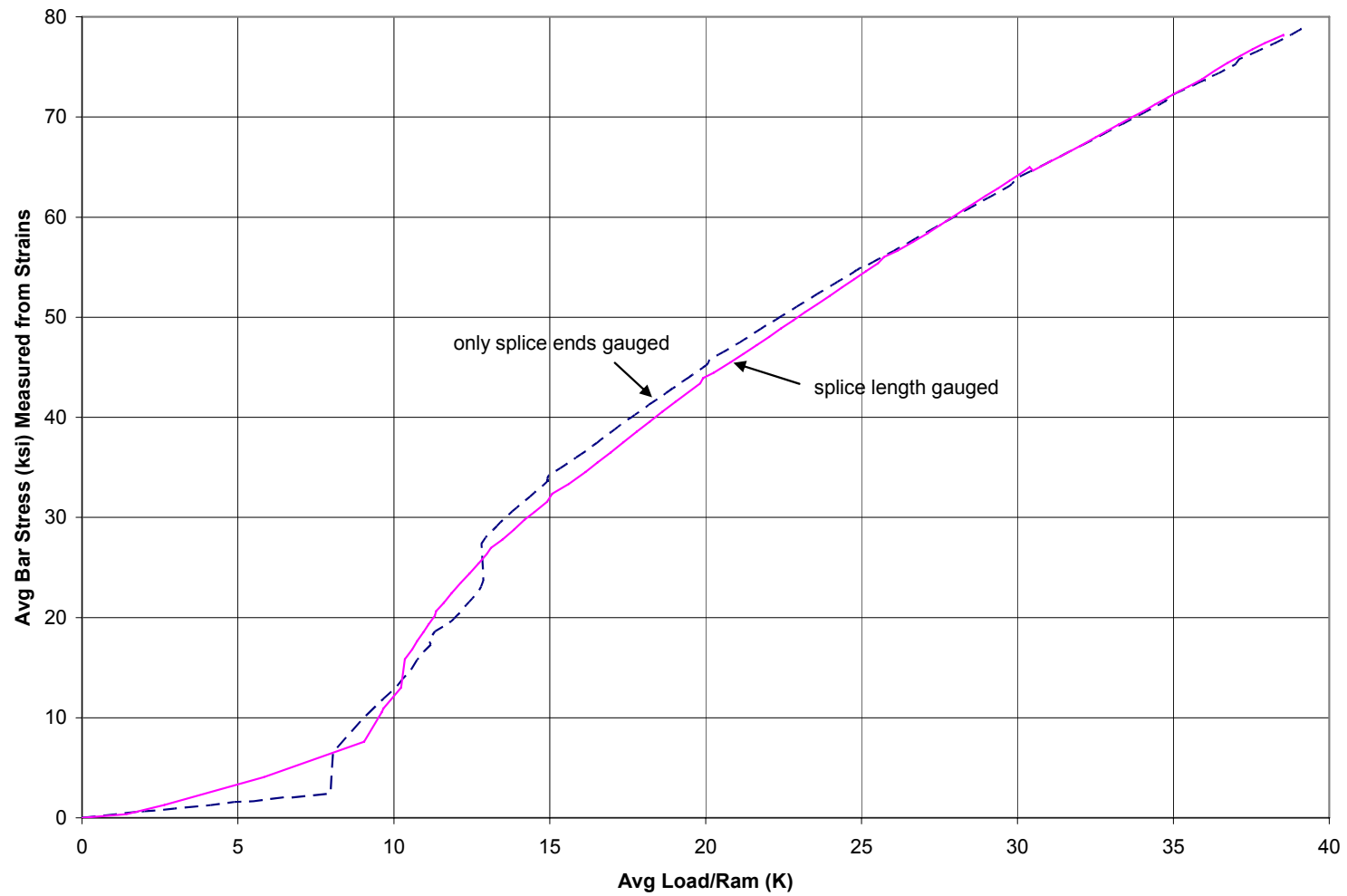Figure 3.9: Comparison of Two Splice Specimens with No Confinement 8-8-OC0 (Ends of Splice Gauged Only) to 8-8-2-OC0 (Splice Fully Gauged) Bar Stress at End of Splice
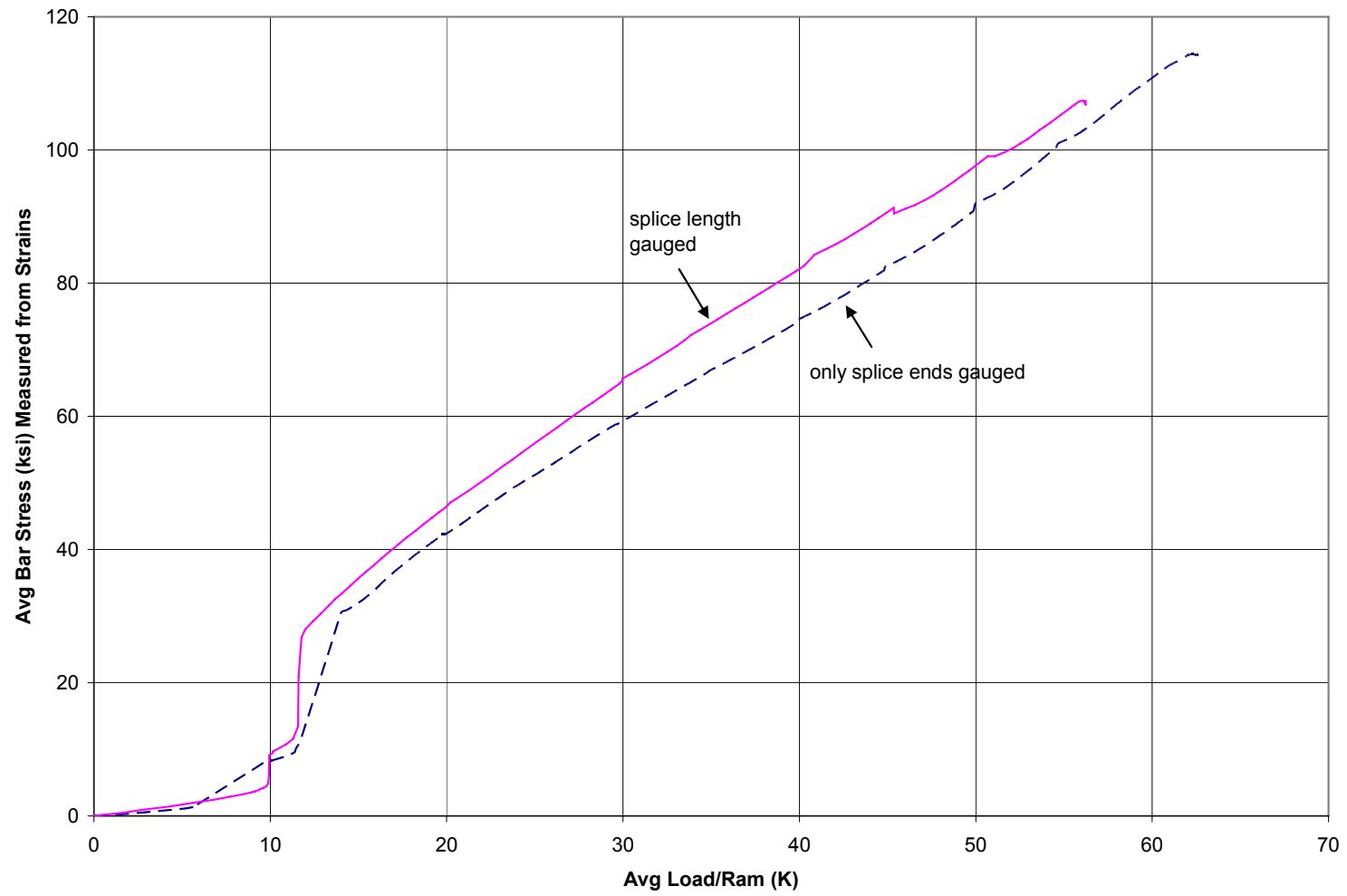
Figure 3.10: Comparison of Two Splice Specimens with Light Confinement 8-8-OC1 (Ends of Splice Gauged Only) to 8-8-2-OC1 (Splice Fully Gauged) Bar Stress at End of Splice

3.3.3 Three Splice Tests

The bar stress readings of the two bars creating the exterior splice were averaged into a single "exterior bar" curve, and the same was done with the interior splice stress readings to create an "interior bar" curve. The bar stress variation along the exterior splice and along the interior splice for the three splice specimen with light confinement (No. 4 stirrups at 13.5 in) is shown in Figure 3.11. The bar stress variation for the specimen with heavy confinement (No. 4 stirrups at 7 in) is shown in Figure 3.12. The three splice specimens show similar trends as the two splice specimens. At low stress levels, the stress along the splice is nonlinear, and gradually becomes linear as the specimen approaches failure. There does not appear to be a significant difference between interior and exterior splices.

A comparison of bar stresses along the exterior splice and along the interior splice of the three splice specimen with light confinement to bar stress along the splices with heavy confinement is shown in Figure 3.13. For comparable load ratios, there is virtually no difference between the low and high levels of confinement. The highly confined splice has a higher capacity than the lightly confined splice. At higher load ratios as the stresses increase, more splitting occurs and the steel carries more stress so there is a greater difference between the light and high confined specimens.
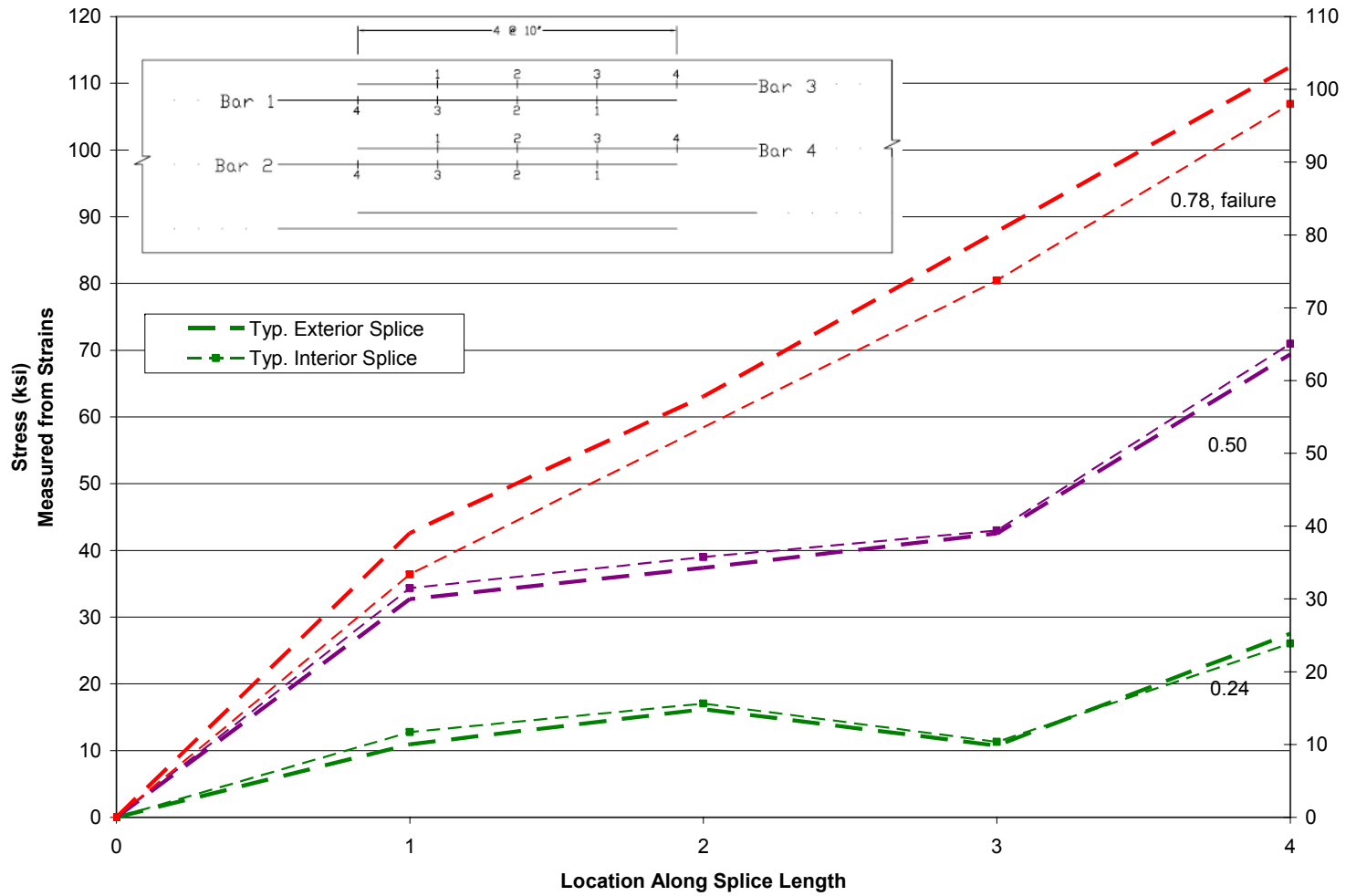
Figure 3.11: Specimen 8-8-3-OC1 Bar Stress Along Exterior Splice and Interior Splice (Light Confinement)

41
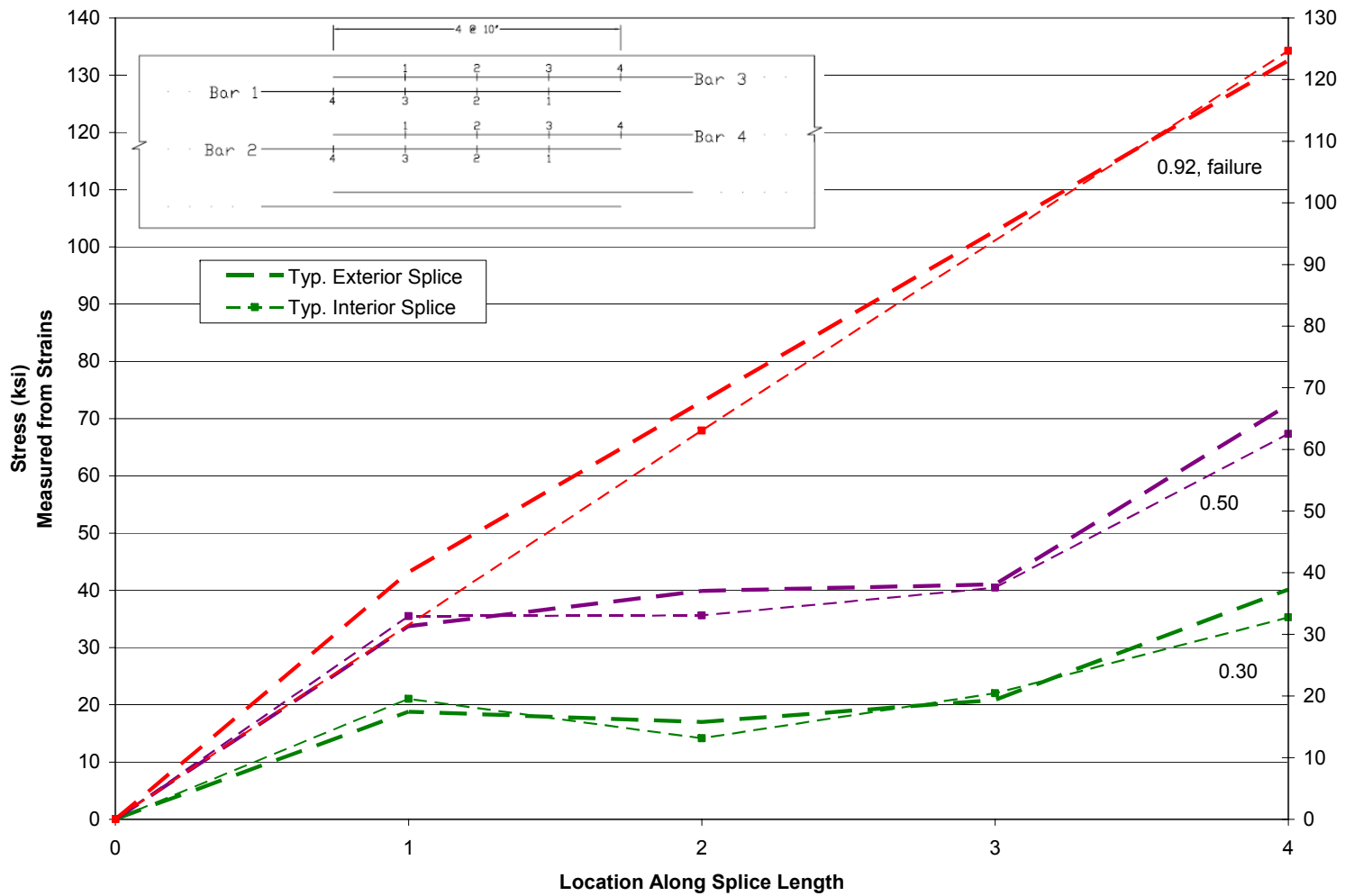
Figure 3.12: Specimen 8-8-3-OC2 Bar Stress Along Exterior Splice and Interior Splice (Heavy Confinement)
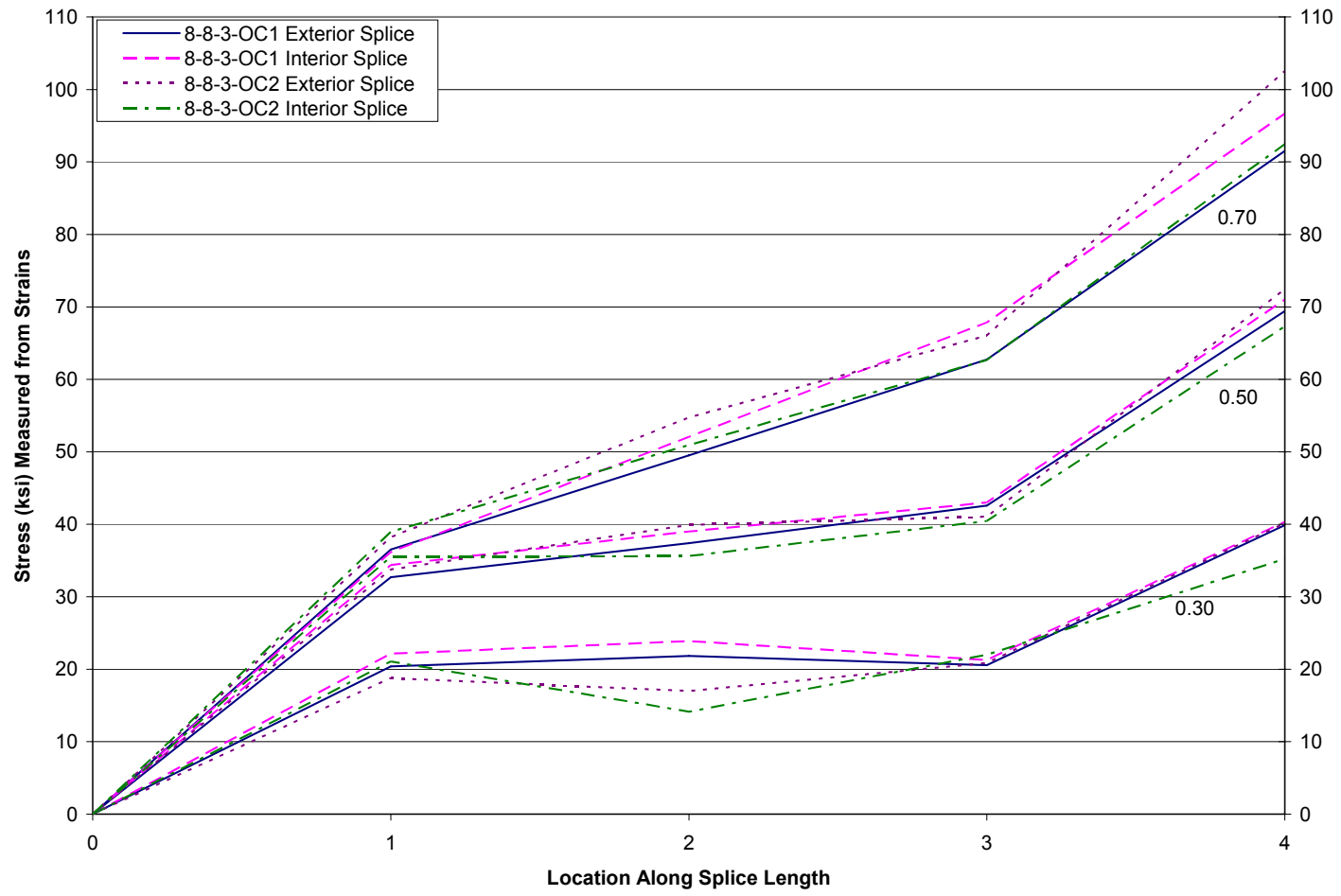
42

Figure 3.13: Comparison of Three Splice Specimens 8-8-3-OC1 (Light Confinement) to 8-8-3-OC2 (Heavy Confinement) Bar Stress Along Splice

Chapter 4: Evaluation of Test Results

4.1 FAILURE MODES

As indicated in Figure 4.1, the two splice and three splice specimens resulted in different splitting planes. Different K_{tr} values would be computed for the two and three splice cases. For a two splice specimen, Figure 1.1(a) and (b) show the two different splitting planes have the same A_{tr}/n value in the K_{tr} term meaning that both splitting planes may occur. Test results shown in Figure 3.1(a) and (b) indicate that the failure mode was a combination of Figure 1.1(a) and (b), face and side splitting.

For the three splice specimen, the different K_{tr} value is based on splitting planes as shown in Figure 1.1(c) and (d). The side splitting mode shown in Figure 1.1(c) results in a lower K_{tr} value than (d) and therefore side splitting is the controlling mode of failure, which is supported by the test results shown in Figure 3.1(c) and (d).

When transverse reinforcement provides large confinement, bar pullout is the mode of failure. To reflect mode of failure, the code sets a limit to the confinement term that includes bar cover and amount of transverse reinforcement. The ACI 408 (Eq. 1-1) limit is 4.0, and the ACI 318 (Eq. 1-2) limit is 2.5. No tests discussed herein resulted in pullout failure although the ACI 318 limit was exceeded in several specimens and a pullout failure did not occur.

4.2 CRACK WIDTHS

In the ACI 318 code, cracking serviceability checks are based on the Gergely-Lutz equation[9]:

$$w = 0.076 \beta f_s \sqrt[3]{d_c A} \qquad \text{(Eq. 4-1)}$$

Where:

w = expected maximum crack width in 0.001 in. units

β = ratio of distances to the neutral axis from the extreme tension fiber and from the centroid of A_s.

f_s = steel stress in ksi

d_c = cover of outermost bar of A_s, measured to the center of the bar

A = tension area per bar measured as the area centered around the c.g. of the tension bars divided by the number of tension bars.

For simplicity, β is often taken as 1.2; however, a β value of 1.1 is more accurate for the beam designs used in these tests. In Figure 4.1, all of the end-of-splice crack width data for the No. 8 specimens in the collaborative test program is plotted and compared with (Eq. 4-1). Again, the nonlinear increase in crack widths with increasing bar stress is clear. At low stress levels, the data points fall within a narrow band, below the line predicted by (Eq. 4-1), and begin to spread as bar stresses exceed about 60 ksi. It is also indicated in Figure 4.1 that crack widths exceed the generally accepted limiting values of 0.013 in. for exterior exposure and 0.016 in. for interior exposure at around 60 ksi. At working stress levels in the serviceability range of 0.6 f_y, conventional Grade 60 steel with a bar stress of 36 ksi is well below the implied code crack width limits. However, at serviceability range for MMFX steel, say f_y = 120 ksi, working stress levels reach 72 ksi; crack widths are well above implied code limits and some data falls above the calculated crack width curve. Reinforcement stressed to high levels (>60 ksi) results in wider cracks. Current codes do not explicitly address cracking at high stresses; however; the bar stress limit of 80 ksi is implemented due to crack width concerns at high stress levels.
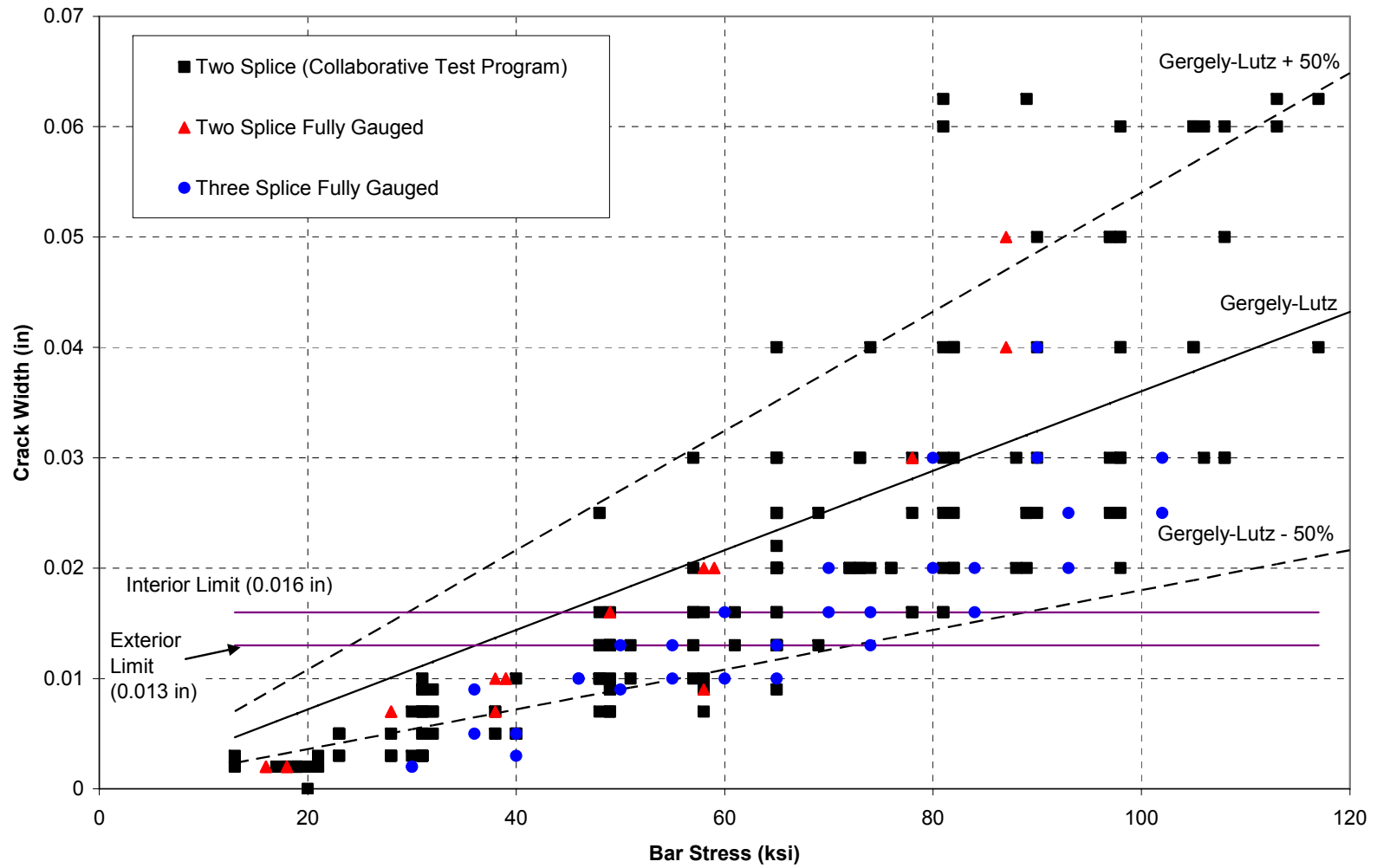
Figure 4.1: Crack Width Data of all Specimens with No. 8 bars (Including Collaborative Test Program)

46

4.3 Comparison of Equations to Experimental Results

The experimental results are compared with values from (Eq. 1-1) and (Eq. 1-2) with $\Phi=1.0$ in Table 4.1. As the splice confinement was increased, the ratio of measured stress to calculated stress (f_{test}/f_{calc}) increased indicating that both equations do not adequately account for splice confinement.

Failure stress computed using ACI 408 (Eq. 1-1) for both two splice specimens without splice confinement was higher than measured, and lower than measured for specimens with confinement.

Failure stress computed using ACI 318 (Eq. 1-2) was higher than measured for every specimen except the three splice specimen with heavy confinement. This suggests that the equation may not be adequate for the high stress levels that can be achieved by MMFX steel. In specimens that reached the pullout failure code limit (2.5) marked with $^+$ in Table 4.1, the f_{test}/f_{calc} ratio is higher than in the specimen where the limit is not reached. For example, for specimen 8-8-2-OC1 with $c_b = 2.0$ in., $K_{tr} = 0.60$, and db = 1.0 the confinement term is:

$$\frac{c_b + K_{tr}}{d_b} = \frac{2 + 0.6}{1} = 2.6 > 2.5 \qquad So\ 2.5\ governs$$

However, with the limited number of tests it is not possible to determine if this is a significant trend.

The average f_{test}/f_{calc} ratio for ACI 408 (Eq. 1-1) is greater than 1.0 and is less than 1.0 for ACI 318 (Eq. 1-2). At high stresses, ACI 408 provides a good estimate of mean failure stresses. It should be noted that ACI 318 (Eq. 1-2) was developed primarily from test data with failure at 60 ksi or less, and has a limit f_y=80 ksi, and was developed for use in design with Grade 60 reinforcement.

47

The interior splice was expected to carry lower stresses than the exterior splice; however test results did not support this hypothesis. To explain the differences between the interior splice and the exterior splice, the two splice specimen is compared to the three splice specimen. Comparing K_{tr} values for a three splice specimen to that of a two splice specimen in Table 4.1, the differences are not large enough to evaluate the limit on K_{tr}. If more tests were to be conducted, three splice specimens should be constructed with the spacing between the interior and exterior splices increased to create a greater difference between the K_{tr} parameters, which is a function of bar cover in both (Eq. 1-1) and (Eq. 1-2).

Test Name	f'c (ksi)	$c_{(ACI\ 408)}$, $c_{b(ACI\ 318)}$ (in)	$(c_*\omega+K_{tr})/d_b$ < 4.0 (ACI408)	$K_{tr\ (ACI\ 408)}$	$(c_b+K_{tr})/d_b$ < 2.5 (ACI318)	$K_{tr\ (ACI\ 318)}$	$f_{experimental}$ (ksi)	(Eq. 1-1) $f_{ACI\ 408}$ (ksi)	(Eq. 1-2) $f_{ACI\ 318}$ (ksi)	$f_{experimental}/f_{ACI408}$	$f_{experimental}/f_{ACI318}$
8-8-OC0*	8.3	2	--	0	--	0	79	81	97	0.98	0.81
8-8-OC1*	8.3	2	2.71	0.71	2.5^+	0.60	114	102	121	1.12	0.94
8-8-2-OC0	7.9	2	--	0	--	0	78	80	95	0.98	0.82
8-8-2-OC1	7.9	2	2.69	0.69	2.5^+	0.60	107	100	119	1.07	0.90
8-8-3-OC1	8.5	2	2.48	0.48	2.40	0.40	105	96	118	1.09	0.89
8-8-3-OC2	8.5	2	2.96	0.96	2.5^+	0.80	129	110	123	1.17	1.05
* Part of collaborative test program									AVG:	1.07	0.90

$^+$Code Limit

Note: All splice lengths, l_d = 40 in, all bar diameters, d_b = 1 in, all factors = 1

Table 4.1: Comparison of Experimental Results to Code Equations

Chapter 5: Summary and Conclusions

5.1 SUMMARY

The test program consisted of six beam specimens with MMFX rebar splices in a constant moment region. Test variables included the use of transverse reinforcement and its spacing, and the number of spliced bars in the beam specimens. In all specimens, the rebar was No. 8, the concrete was 8 ksi, the splice length was 40 in. and the cover was 1.5 in. on all sides of the bar. Specimens with transverse reinforcement involved No. 4 Grade 60 ties.

The splice lengths were instrumented with strain gauges to monitor bar stress distribution along the splice length. Four of the beam specimens included two spliced rebars, with two of those specimens part of a collaborative test program mandating strain gauges on splice ends only. The remaining two specimens consisted of three spliced rebars.

5.2 CONCLUSIONS

Based on test observations, the following conclusions are made:

1. The development length equation in ACI 318-05 was not adequate at the high stresses at which the confined splices with MMFX steel failed. The ACI 408 equation provided a good estimate of mean failure stresses at high stresses. Both equations predicted lower strengths than measured in specimens with confinement.

2. The bar stress distribution along the splice length was nonlinear at low stress levels, but as the splice nears failure, the bar stress distribution was linear along

the splice length. The linear nature of the current development length code equation is acceptable.

3. In the three splice specimens, the behavior of the interior splice was nearly identical to that of the exterior splice. Two specimens were tested with three splices with different levels of confinement, and one resulted in the exterior splice carrying more stress than the interior splice at failure and the second test resulted in the opposite conclusion.

4. High steel stresses resulted in greater crack widths than currently acceptable for service load stresses using Grade 60 steel. The equation used to determine serviceability limits only appears to be effective for stress levels of 60 ksi or less.

5. There did not appear to be a difference in bond behavior between the specimens with fully gauged splices and those with gauges on splice ends only. Since splitting controlled failure, the tightly wrapped tape that was used to seal the strain gauge did not reduce the restraint of the cover concrete and the remaining lugs were sufficient to produce splitting.

References

1.   ACI Committee 318, *Building Code Requirements for Structural Concrete (ACI 318-05)*, American Concrete Institute, Farmington Hills, Mich., 2005.

2.   ACI Committee 408, *Bond and Development of Straight Reinforcing Bars in Tension (ACI 408R-03)*, American Concrete Institute, Farmington Hills, Mich., 2003.

3.   Ahlborn, T., and DenHartigh, T., "A Comparative Bond Study of MMFX Reinforcing Steel in Concrete," Michigan Tech University, Center for Structural Durability, Houghton, MI, 2002.

4.   El-Hacha, R.; El-Agroudy, H.; Rizkalla, S., "Bond Characteristics of High-Strength Steel Reinforcement," *ACI Structural Journal*, V. 103, No. 6, Nov.-Dec. 2006, pp. 771-782.

5.   Malhas, F., "Preliminary Experimental Investigation of the Flexural Behavior of Reinforced Concrete Beams Using MMFX Steel," University of North Florida, Jacksonville, FL, 2002.

6.   Thompson, M.A.; Jirsa, J.O.; Breen, J.E.; Meinheit, D.F., "Behavior of Multiple Lap Splices in Wide Sections," *ACI Journal*, Feb. 1979, pp. 227-248.

7.   Orangun, C.O.; Jirsa, J.O.; Breen, J.E., "A Reevaluation of Test Data on Development Length and Splices," *ACI Journal*, March 1977, pp. 114-122.

8.   Glass, G.M., "Performance of Tension Lap Splices with MMFX High Strength Reinforcing Bars," Unpublished Thesis, The University of Texas at Austin, to be published 2007.

9.   Gergely, P. and Lutz, L. A., "Maximum Crack Width in Reinforced Concrete Flexural Members," Special Publication SP-20, *American Concrete Institute*, 1968, pp.87-117.

Vita

Kathryn Diane Hoyt was born in San Antonio, TX on December 30, 1982 to John and Mari Hoyt. She has one older sister, Angie. After graduating from John Marshall High School, she attended The University of Texas at San Antonio. She received her Bachelor of Science in Civil Engineering in December 2004. She then worked as an engineer in training at Baker Engineering and Risk Consultants. In August 2005 she began her graduate studies at The University of Texas at Austin working as a research assistant at the Phil M. Ferguson Structural Engineering Laboratory. She will receive her Master of Science in May 2007 under the direction of Dr. James O. Jirsa.

Permanent address: 7035 Forest Mont

San Antonio, Texas 78240

This dissertation was typed by the author.